A NOVEL BIOSENSOR FOR DIRECT ANTIBODY DETECTION BASED ON THE ANTIBODY-CATALYZED WATER OXIDATION PATHWAY

A Thesis

Presented to the Faculty of the Graduate School

of Cornell University

In Partial Fulfillment of the Requirements for the Degree of

Master of Science

by

PRANAV SUNDARAM

AUGUST 2018

ABSTRACT

Current medical practice to diagnose Lyme Borreliosis involves observation of symptoms combined with serological detection of antibodies against *Borrelia* antigens using ELISA and Western blotting. These methods detect the captured serum antibodies by using secondary reagents that present certain limitations such as non-specific binding leading to false positives, species-specificity, time-intensive incubation steps and increased cost.

We report a novel biosensor based on the antibody-catalyzed water oxidation pathway (ACWOP), that directly detects captured antibodies by using their intrinsic catalytic property and generates an antibody-dependent colorimetric signal. The sensor uses inexpensive porous silica microparticles functionalized with an antigen and other ACWOP cofactors to capture specific antibodies on a surface and detect them via the ACWOP.

By eliminating secondary reagents, our sensor acts as a species-independent and inexpensive platform that aids in transitioning to our ultimate goal of developing a point-of-care device for widespread monitoring of Lyme disease across multiple hosts.

BIOGRAPHICAL SKETCH

Pranav Sundaram is currently a 2nd year Master of Science student in the Chemical and Biomolecular Engineering department at Cornell University.

He earned his Bachelor of Technology degree in Chemical Engineering from the National Institute of Technology - Tiruchirappalli (NIT) in India and graduated First Class with Distinction. During his freshman year, he won the Mitacs Globalink Research Internship Award to pursue a 12-week long internship in McMaster University, Canada, where he worked on developing microfluidic bioreactors for culturing cells. The internship introduced him to the field of microfluidics, point of care diagnostics and biosensors that became his primary research interests.

Mr. Sundaram was part of the R&D club at NIT, where he conducted workshops and taught basic electronics to more than 300 college students. He actively participated in technical competitions and has won awards such as the Winning Team at Wipro Earthian'14, Young Innovator Award at Shell Ideas 360 for designing a smart tap and 3rd place at NIT's Technical Exhibition Event for developing a 25$ smart watch. He has held several positions of responsibility which include Teaching Assistant at Cornell University, Event Manager at NIT's Technical Festival and Club Inductions Head at NIT's R&D Club.

ACKNOWLEDGMENTS

I would first like to express my sincere gratitude to my thesis advisor Prof. Brian Kirby for his continuous support during my research project and for his patience, motivation and immense knowledge. He allowed me to conduct my research independently and steered me in the right direction whenever he thought I needed it. His door was always open and I received valuable advice from him on a variety of topics ranging from research and course-related technical questions to career advice and professional development.

I would also like to thank my other research committee members Prof. Christopher Ober and Prof. Abraham Stroock. They provided me with insightful comments and encouragement and helped me think about my research from various perspectives.

My sincere thanks also goes to Andrew Sanchez and Roselynn Cordero, my project-mates, for the stimulating discussions and constant support they provided me with throughout my Masters study at Cornell. Without their input, it would not have been possible to conduct this research.

Last but not the least, I would like to thank my parents and my sister for their constant motivation and support that provided me the drive to complete my project successfully.

TABLE OF CONTENTS

CHAPTER 1

INTRODUCTION

Lyme disease or Lyme Borreliosis is the fastest growing vector-borne disease in the United States, with more than 300,000 people infected annually, as of 2014 [1]. The bacterium that causes the disease, *Borrelia burgdorferi*, is primarily transmitted by black-legged ticks which acquire the pathogen from reservoir hosts, such as rodents and birds. Lyme disease affects a number of additional hosts, such as humans, wildlife, pets and livestock, and it is critical to monitor the disease across species to manage prevalence and detect the infection early. The most distinctive symptom, erythyma migrans (bullseye rash), does not develop for every infected patient, and secondary symptoms such as fever, fatigue and myalgia mimic 300 other diseases. This makes symptom-based diagnosis difficult for Lyme Disease. If the disease is left untreated for long, it develops into Chronic Lyme Disease (CLD), which can lead to paralysis and nerve damage [2]. A recent study showed that CLD patients reported a significantly lower health quality status, for both mental and physical health when compared to other chronic health conditions [3].

The bacterium enters through the skin and makes its way to the heart, tissue and joints, making serological detection of the *Borrelia* antigen unreliable and difficult [4]. Hence current standard medical practice is to diagnose Lyme disease by observation of symptoms combined with serological detection of the host's antibodies against *Borrelia* antigens using an Enzyme Linked Immuno-Sorbent Assay (ELISA) and confirmation by - Western Blotting [5]. Both methods detect the primary

antibodies captured from serum using secondary reagents that exhibit non-specific binding and lead to false positives [6]. Further, these specially prepared secondary reagents are expensive and specific to the species being tested for, thereby making cross-species detection of the disease with the same test difficult [7].

We make use of the native catalytic property of the captured primary antibodies to directly detect them, thereby eliminating the use of secondary reagents and any limitations associated with them. Wentworth et. al. showed that all antibodies, irrespective of specificity, class or species, can catalyze the reaction between singlet oxygen and water to generate hydrogen peroxide, a process called the antibody-catalyzed water oxidation pathway, or ACWOP [8].

Our ultimate goal is to develop a point-of-care sensor using a lateral flow test format that can detect Lyme antibodies from serum against specific *Borrelia* antigens (OspA, OspC and OspF) directly via ACWOP. Such a device can help monitor Lyme disease in multiple species and understand disease progression better. Additional applications for an ACWOP biosensor could include analyzing seroconversion dynamics in multiple species and testing vaccine efficacy by measuring antibody responses [9, 10].

As an important step towards achieving this ultimate goal, we demonstrate a novel, species-independent and inexpensive platform that detects primary immunocaptured antibodies directly via ACWOP and generates antibody-dependent colorimetric readout. This enables smooth transition to a point-of-care sensor that can achieve widespread monitoring of Lyme disease across hosts.

CHAPTER 2

Article

A novel biosensor for direct antibody detection based on the antibody-catalyzed water oxidation pathway

Pranav Sundaram [1], Roselynn Cordero[2], Andrew Sanchez [1], Wei-Liang Chen[1], Christopher K. Ober[1,3] and Brian J. Kirby [1,4,5,*]

[1] Robert Frederick Smith School of Chemical and Biomolecular Engineering, Cornell University, Ithaca, NY

[2] Department of Chemistry and Chemical Biology, Cornell University, Ithaca, NY

[3] Department of Material Science and Engineering, Cornell University, Ithaca, NY

[4] Sibley School of Mechanical and Aerospace Engineering, Cornell University, Ithaca, NY

[5] Department of Medicine, Division of Hematology and Oncology, Weill-Cornell Medicine, NY, NY

Abstract: Infectious diseases affect a number of hosts and present a constant threat of developing into epidemics. Current clinical diagnosis of infectious diseases is performed using an Enzyme Linked Immuno-Sorbent Assay (ELISA) that makes use of secondary reagents to detect primary antibodies captured from serum. Use of these secondary reagents can cause limitations, such as false positives (due to non-specific binding), time-intensive incubation steps, species-dependence and increased cost. To overcome these limitations, we report a novel biosensor based on the antibody-catalyzed water oxidation pathway (ACWOP) that directly detects captured primary antibodies by using their inherent catalytic activity. In this process, antibodies are

* Correspondence: kirby@cornell.edu

Author contributions listed on page 29.

used as catalysts in the reaction between singlet oxygen and water to generate hydrogen peroxide, which is then detected via colorimetric readout. Our sensor incorporates silica microparticles as an inexpensive substrate that is functionalized with rose bengal (photosensitizer), to generate singlet oxygen, and dinitrophenyl (antigen), to capture primary antibodies. We demonstrate specific capture of anti-DNP antibodies on our substrates followed by generation of an antibody-dependent colorimetric ACWOP signal. By eliminating the use of secondary reagents, we have developed a universal platform that detects antibodies in a species-independent manner with improved speed and inexpensive reagents, with the ultimate goal of transitioning to a point-of-care sensor that can be used for widespread monitoring of infectious diseases.

Keywords: ACWOP, biosensor, point-of-care, infectious disease monitoring, direct antibody detection, ELISA, species-independence

1. Introduction

Infectious diseases affect a number of hosts such as humans, livestock, pets and wildlife [1]. For example, the influenza virus resides in reservoir hosts, such as ducks, cranes and other wild birds, from which the pathogen then passes into transmission hosts, such as domestic poultry and bats and ultimately to spillover hosts such as humans, cows, cats and swine [2,3]. Infectious diseases spread rapidly and pose the threat of developing into epidemics that can cause large scale loss of lives [4-6]. Several key factors aid in the spread of infectious diseases: multiple species acting

as transmission and spillover hosts, increased contact between humans and wildlife and other species, frequent travelling across nations and lack of global monitoring strategies [7]. Hence it is important to develop novel sensitive tools that can achieve widespread monitoring of these diseases across several species in a timely manner [8].

Currently, serology is the primary clinical tool used for detecting infectious pathogens in several hosts. In serology, antibodies that are developed as part of the host's immune response to the infection are detected in the patient's serum. These disease-specific antibodies have a unique function of binding to a specific molecule on the target pathogen (i.e. the antigen), and hence their presence in the patient's serum can indicate exposure to pathogen.

The Enzyme Linked Immuno-Sorbent Assay or ELISA is the most commonly used in-vitro diagnostic test to detect antibody responses to infectious agents in the host [9]. In an ELISA, the host's serum is incubated in antigen-coated microwell plates. Antibodies specific to the coated antigen are captured from the patient's serum onto the plates through antigen-antibody binding [10]. These captured primary antibodies are then detected with secondary reagents. Based on the secondary reagent used, ELISAs are classified into two types: indirect ELISA and competitive ELISA. An indirect ELISA uses secondary antibodies that are tagged to an enzyme such as horseradish peroxidase (colorimetric detection) or a fluorophore (fluorometric detection). These secondary antibodies are species-specific, as they recognize the Fc fragment of the captured primary antibody. On the other hand, a competitive, or c-ELISA, uses antibodies that compete with primary antibodies from serum for the

antigen binding sites. These competitive antibodies are species-independent and are antigen-specific.

Use of secondary reagents present certain limitations: (a) non-specific binding of secondary reagents in the wells can lead to false positives and low sensitivity [11], (b) additional incubation steps, which range from 2 hours at room temperature to overnight at $4^{O}C$, are required for binding these secondary reagents, thereby increasing the total test time [10], (c) the use of secondary antibodies that are specific to the species being tested for prevents testing across several hosts with the same device [12] and (d) the use of secondary reagents increases the overall cost of the tests [13].

To overcome these limitations, we eliminate use of secondary reagents by directly detecting the captured primary antibodies using their intrinsic catalytic property. Wentworth et. al. showed that all antibodies, irrespective of antigenic specificity or source, can act as a catalyst in a specific reaction between singlet oxygen($^{1}O_2$) and water to form hydrogen peroxide (H_2O_2) [14]. This process is termed the antibody-catalyzed water oxidation pathway, or ACWOP. They tested a panel of intact immunoglobulins and antibody fragments from a range of species, clones and isotypes and found this property to be conserved across all antibodies [15]. The catalytic active site has been proposed to exist in the inter-greek key domain interface between the light and heavy chains, which stabilizes the H_2O_3 intermediate formed during this reaction [16, 17].

We engineered a surface-based biosensor that uses porous silica microparticles as an inexpensive substrate for functionalizing cofactors required for the ACWOP and

antigens required for capturing primary antibodies. The captured primary antibodies generate H_2O_2 via the ACWOP, which is detected and quantified using a colorimetric method. Our sensor successfully generates an antibody-dependent ACWOP signal with fewer incubation steps and cheaper reagents. Through the development of this universal platform, we demonstrate potential to transform our biosensor into a species-independent point-of-care device that can be used for rapid, cheap and sensitive monitoring of infectious diseases across a host of species.

2. Materials and Methods

2.1. Materials:

Hydrogen peroxide (Cat: 216763), Peroxidase from horseradish (HRP, Cat: P8125-25KU), 3,3′,5,5′-Tetramethylbenzidine (TMB, Cat: 860336), Hydrochloric acid (Cat: 435570), Toluene (Cat: 244511), N,N-Dimethylformamide (Cat: 227056), HATU (Cat: 445460), N,N-Diisopropylethylamine (Cat: D125806), DNP-ε-amino-n-caproic acid (Cat: D7754), 1,4-Dimethylpyridinium p-toluenesulfonate (Cat: 514888), DIC (Cat: D125407), TWEEN-20 (Cat: P9416) and Citric Acid (CAS: 77-92-9) were purchased from Millipore Sigma. Rose Bengal (CAS: 632-69-9, Stock: A17053) and porous silica gel (CAS: 63231-67-4, Stock: 42726) were purchased from Alfa Aesar. 1x Dulbecco's Phosphate-Buffered Saline (DPBS, Cat: 45000-434), Methanol (Cat: BDH2029), Ethanol (Cat: 89125-188), L(+)-Ascorbic acid (Cat: 200000-052), Triethylamine (Cat: 200001-372), Sodium phosphate dibasic (Cat: JT4062-1) and Dimethyl sulfoxide (Cat: 97061-250) were purchased from VWR International. 3-Aminopropyl (diethoxy) methylsilane (CAS: 18306-79-1) was purchased from Gelest.

Rose Bengal Disodium Salt (Cat: R323-25) was purchased from Fisher Scientific. Clear F-bottom 96-well microplate (Cat: 651101) and Black F-bottom 96-well microplate (Cat: 655076) were purchased from Greiner Bio-one. Normal Rat IgG, Azide free (Cat: 6-001-F) was purchased from R&D Biosystems, Goat anti-DNP IgG (Cat: A150-117A) was purchased from Bethyl Laboratories and Donkey anti-goat IgG-Alexa Fluor 568 (Cat: A-11057) was purchased from ThermoFisher Scientific. Dinitrophenyl mouse IgG (Cat: sc-69697) and Normal-mouse IgG (Cat: sc-2025) were purchased from Santa Cruz Biotechnology.

TMB stock solution: Citrate Phosphate (CP Buffer, pH 5.0) was prepared by mixing 24.3mL of 0.1N citric acid, 25.7mL of 0.2N sodium phosphate and 50mL of DI water. TMB stock solution of 1.04mM was prepared by adding 5mg of TMB powder to 5mL DMSO and stirred gently until TMB dissolved. The prepared solution was then added to 15mL CP buffer.

Unless otherwise stated, all stock solutions were prepared by dilution or dissolution in 1x DPBS.

2.2. Equipment:

A Synergy H1 Hybrid plate reader from BioTek was used at default settings to measure absorbance intensity, absorbance spectra, and fluorescence intensity of samples. BioTek Gen5 data analysis software was used to analyze optical data collected from the plate reader. A Sorvall ST16 centrifuge from ThermoFisher Scientific fitted with a swinging bucket rotor-Model: M20 for 96-well microplates and Model: TX-400 for Falcon tubes, was used to wash substrates. A Centrifuge 5424

from Eppendorf fitted with a fixed angle (45^o) rotor - Model: FA-45-24-11 was used for microcentrifugation. A Select Series UV Crosslinker (XLE-1000A) from Spectroline was repurposed with four 12" green cold cathode tube lights from Logisys (CLK12GN2, brightness: 28000 to 30000 cd/m^2) to form a green-light illuminator. The green lights were controlled with an external HY3003 DC power supply at 12V and 1.25A with a toggle switch. The green light illuminates a region suitable for placing a 96-well microplate. A Vacuum filtration unit was designed by fitting vacuum tubing to an Erlenmeyer flask and attaching a 60mL Pore-E buchner funnel at the top.

2.3. Detection of singlet oxygen generated by photosensitization reaction in solution:

Rose Bengal was diluted in DPBS (pH 7.4, 100µL) to form the following concentrations: 6.25µM, 5µM, 4µM, 3.12µM, 2µM and 1.56µM and was added to wells 1-6 in Row A in a clear 96-well microplate. A negative control of DPBS (pH 7.4, 100 µL) was added to well 7 in Row A. Ascorbic Acid (100µL, 0.625mM stock) was added to all 7 wells. The plate was placed in the green-light illuminator and illuminated from above for 30 minutes. HRP (20µL, 0.171µM stock) and TMB (100µL, 1.04mM stock) were added to each well. The plate was covered with aluminium foil and incubated for 5 minutes. The absorbance intensity at 650nm was measured for each well in the plate reader. The above experiment was performed in triplicate and each data point is reported as the mean $\pm$ S.E.M. The absorbance intensity at 650nm was converted to [H_2O_2] using the H_2O_2 standard curve.

2.4. Proof of concept ACWOP assay in solution - all reagents freely diffusing in solution:

Rat IgG, azide free, that was resuspended in DPBS (100µL, 20µM stock) was serially diluted in DPBS (pH 7.4, 100µL) with a dilution factor of 1/2 in 11 wells of a clear 96-well microplate. A well containing DPBS (pH 7.4, 100µL) was used as the negative control. RB (100µL, 0.01mM) was added to all 12 wells. The plate was placed in the green-light illuminator and illuminated from above for 30 minutes. HRP (20µL, 0.171µM stock) and TMB (100µL, 1.04mM stock) were added to each well. The plate was covered with aluminium foil and incubated for 5 minutes. The absorbance intensity at 650nm was measured for each well in a plate reader. The above experiment was performed in triplicate and each data point is reported as the mean $\pm$ S.E.M. The absorbance intensity measured was converted to [H_2O_2] using the H_2O_2 standard curve.

2.5. Functionalization of Rose Bengal on silica microparticles:

2.5.1. Activation of silica microparticles:

12g of silica microparticles were mixed with 100mL of 10% HCl (10mL HCl to 90mL water) and refluxed with continuous stirring for 24 hours at 110˚C. After 24 hours, the silica microparticles were collected by filtration and decantation, washed with pure water until the pH of the water was neutral, and dried at 60˚C for 24 hrs.

2.5.2. APDMES conjugation on silica microparticles:

The dried particles (11g) were then added to a 300mL round-bottom flask along with 100mL of anhydrous toluene, 4.5mL of APDMES, and 2.5mL of triethylamine. This mixture was refluxed at 110˚C for 24 hours. Subsequently, the mixture was left to cool to room temperature and particles were collected by filtration. The silica microparticles were washed with methanol and ethanol 5 times each. The APDMES-silica microparticles were then dried in an oven for 24 hours.

2.5.3. Rose Bengal Conjugation on APDMES-silica microparticles:

The concentration of Rose Bengal used was 2mM (Rose Bengal: 1 equivalent, HATU: 1 equivalent, DIPEA: 2 equivalents). 2g of APDMES-silica microparticles was added to a 100mL round-bottom flask along with 30mL of amine-free anhydrous DMF and a stir bar. 61.06 mg of Rose Bengal sodium salt, 22.82mg of HATU (coupling agent) and 21μL of N, N-Diisopropylethylamine (DIPEA base) was added to the mixture and stirred manually for about 1 minute. This solution was stirred for 24 hours at room temperature, collected via filtration, and washed with methanol, ethanol, and DPBS buffer solution until mother liquor was colorless.

2.6. Detection of singlet oxygen generated by photosensitization reaction on a surface:

2.6.1. Detection with Ascorbic Acid:

RB-functionalized silica microparticles (RB-silica) were suspended in DPBS (pH 7.4) to obtain a concentration of 15mg RB-silica per 100µL of suspension. The same was done for APDMES-silica microparticles for the negative control. RB-silica suspension (100µL, 15mg per 100µL of suspension) and APDMES-silica suspension (100µL, 15mg per 100µL of suspension) was added wells in a clear 96-well microplate. Ascorbic acid (100µL, 78µM stock) was added to both wells. The plate was placed in the green-light illuminator and illuminated from the top for 30 minutes. 150µL of the supernatant from each well was collected in individual microcentrifuge tubes. The tubes were centrifuged in a microcentrifuge at 18000xg for 5 minutes. 100µL of the supernatant from the tubes were then transferred to a new clear 96-well microplate. An absorption spectrum was performed for both wells to ensure that there was no freely diffusing RB in solution. HRP (20µL, 0.171µM stock) and TMB (100µL, 1.04mM stock) were then added to each well. The plate was covered with aluminium foil and incubated for 5 minutes. The absorbance intensity at 650nm was measured for each well. The above experiment was performed in triplicate and each data point is reported as the mean $\pm$ S.E.M. The absorbance intensity at 650nm was converted to $[H_2O_2]$ using the H_2O_2 standard curve.

2.6.2 Detection with freely diffusing IgG:

RB-functionalized silica microparticles (RB-silica) was suspended in DPBS (pH 7.4) to obtain a concentration of 15mg RB-silica per 100µL of suspension. Rat IgG, azide free, resuspended in DPBS (100µL, 15.87µM stock) was serially diluted in DPBS (pH 7.4, 100µL) with a dilution factor of 1/2 in 10 wells of a clear 96-well

microplate. A well containing DPBS (pH 7.4, 100µL) was used as the negative control. The remaining procedure was the same as described in 2.6.1.

2.7. Functionalization of Dinitrophenyl on silica microparticles:

0.3g of APDMES-silica microparticles (protocol in 2.6) were added to a 50mL round-bottom flask equipped with a stir bar along with 10mL of amine-free anhydrous DMF. Then, 18.75mg of DNP, 93.75 mg of 1,4-Dimethylpyridinium p-toluenesulfonate (DPTS), and 62.5µL of N,N′-Diisopropylcarbodiimide (DIC) were added to the flask with the particles. This solution was stirred at 32˚C for 24 hours. The particles were then washed with ethanol and methanol using several centrifugation steps until the supernatant was clear. The washed particles were dried in the oven at 60˚C for two hours.

2.8. Capture of primary anti-DNP IgG on DNP functionalized silica microparticles - Readout with fluorophore-tagged secondary antibodies:

DNP-functionalized silica microparticles (DNP-silica) were suspended in DPBS (pH 7.4) to obtain a concentration of 30mg DNP-silica per 100µL of suspension. Goat anti-DNP IgG (100µL, 6.67µM stock) was serially diluted in DPBS (pH 7.4, 100µL) with a dilution factor of 1/2 in 11 wells of a clear 96-well microplate. A well containing DPBS (pH 7.4, 100µL) was used as the negative control. DNP-silica suspension (100µL, 30mg per 100µL of suspension) was added to all 12 wells. The plate was covered with aluminium foil and incubated for 4 hours at room temperature (25^{o}C). Wash buffer (200µL, 0.05% (v/v) Tween-20 in DI) was added to each well. The plate was centrifuged at 3000xg for 3 minutes and the resulting

supernatant was aspirated. The wash protocol described was performed 3 times. AlexaFluor 568 donkey anti-goat IgG (100µL, 0.01µM) was added to all 12 wells. The plate was covered with aluminium foil and incubated for 2 hours at room temperature (25^{o}C). The wash protocol described was performed 3 times. DPBS (100µL, pH 7.4) was added to each well and all of the contents of each well were transferred to a black 96-well microplate. The fluorescence intensity (Ex: 568nm, Em: 603nm) was measured for each well using a plate reader. The above experiment was performed in duplicate and each data point is reported as the mean $\pm$ S.E.M.

2.9. Demonstration of a surface-based antibody sensor that directly detects captured primary antibodies via the ACWOP:

2.9.1. ACWOP readout of captured primary anti-DNP antibodies:

DNP-functionalized silica microparticles (DNP-silica) were suspended in DPBS (pH 7.4) to obtain a concentration of 15mg DNP-silica per 100µL of suspension. RB functionalized silica microparticles (RB-silica) was suspended in DPBS (pH 7.4) to obtain a concentration of 15mg RB-silica per 100µL of suspension. Mouse anti-DNP IgG (100µL, 1.33µM stock) was serially diluted in DPBS (pH 7.4, 100µL) with a dilution factor of 1/2 in 7 wells of a clear 96-well microplate. A well containing DPBS (pH 7.4, 100µL) was used as the negative control. DNP-silica suspension (100µL, 15mg per 100µL of suspension) was added to all 8 wells. The plate was covered with aluminium foil and incubated for 4 hours at room temperature (25^{o}C). Wash buffer (200µL, 0.05% (v/v) Tween-20 in DI) was added to each well. The plate was centrifuged at 3000xg for 3 minutes and the resulting supernatant was

aspirated. The wash protocol described was performed 3 times. RB-silica suspension (100µL, 15mg per 100µL of suspension) was added to all 8 wells. The plate was placed in the green-light illuminator and illuminated from the bottom for 45 minutes. 150µL of the supernatant from each well was collected in individual microcentrifuge tubes. The tubes were centrifuged in a microcentrifuge at 18000xg for 5 minutes. 50µL of the supernatant from the tubes were then transferred to a new clear 96-well microplate. An absorption spectrum was performed for all 8 wells using a plate reader to ensure there was no freely diffusing RB in solution. HRP (20µL, 0.171µM stock) and TMB (100µL, 1.04mM stock) were then added to each well. The plate was covered with aluminium foil and incubated for 5 minutes. The absorbance intensity at 650nm was measured for each well in a plate reader.

2.9.2. ACWOP readout of captured primary control antibodies:

N-Mouse IgG (100µL, 2.67µM stock) was serially diluted in DPBS (pH 7.4, 100µL) with a dilution factor of 1/2 in 6 wells of a clear 96-well microplate. Same procedure as 2.9.1 was followed and instead of Mouse anti-DNP IgG, a control antibody was used to determine non-specific binding of IgG to silica microparticles.

3. Results and Discussion

The key components of our ACWOP biosensor include silica microparticles used as an inexpensive substrate to conjugate antigens and ACWOP cofactors, $^1O_2$ (reactant) generation on a surface and an optimized colorimetric detection system to detect the H_2O_2 generated via antibody catalysis.

We used a TMB-HRP based colorimetric detection system to detect the generated H_2O_2. On oxidation by stock H_2O_2, TMB changed from colorless to blue in the presence of an enzyme HRP [18]. This change in color was detected and quantified by measuring absorbance at 650nm using absorbance spectroscopy with a plate reader. The colorimetric detection signal was expressed as the Absorbance intensity or OD at 650nm/Path Length, with a linear trend against H_2O_2 concentration. We optimized the detection system for [HRP] and [TMB] to obtain a final H_2O_2 standard curve. Our system developed a colorimetric detection signal of H_2O_2 within 5 minutes, not shown previously in literature, with a sensitivity of 0.078μM (data in Appendix A.1). We obtained a relationship between the measured colorimetric intensity signal and [H_2O_2], which was used for conversion in all further experiments.

Singlet oxygen, the excited state of molecular oxygen, is a key reactant in the ACWOP reaction and was generated via a photosensitization reaction [19]. The process required oxygen, light of a suitable wavelength and a photosensitizer that can absorb that light and use its energy to excite oxygen to its singlet state. We used the xanthene dye, Rose Bengal (RB) as the photosensitizer primarily for three main reasons: (a) it has a high quantum yield of 0.76, (b) it is soluble and can be used to photosensitize in DPBS and (c) it is inexpensive [19]. RB has an absorption maximum at 550 nm (Fig S1), i.e green light, so we designed an illuminator system (Fig 1a) to provide a constant and uniform source of green light.

Although the final readout uses ACWOP, to initially quantify the $^1O_2$ generated by photosensitization of RB with green light, we used an ascorbic-acid

detection system. Ascorbic acid (AA) reacts with $^1O_2$ in a 1:1 mole ratio to generate H_2O_2 at a pH of 7.4 [20]. The generated H_2O_2 was detected with our optimized TMB-HRP colorimetric detection system. AA dissolved in 1x DPBS (10mM phosphate/160mM sodium chloride, pH 7.4) showed a decrease in pH below 7.4 for [AA] > 10mM (Fig S2). For [AA] < 10mM, the generation of $^1O_2$ as a function of [AA] showed an ascorbate dependent detection signal. There existed an optimal [AA] for both RB freely diffusing in solution and RB functionalized on silica microparticles (Fig S3, S4). Detection of $^1O_2$ generated due to photosensitization reactions in solution, using the optimum [AA], showed a linear increase in $^1O_2$ generated with [RB] (Fig 1b). A minimum of [RB] = 0.78μM was required to generate detectable $^1O_2$ in solution for the given conditions.

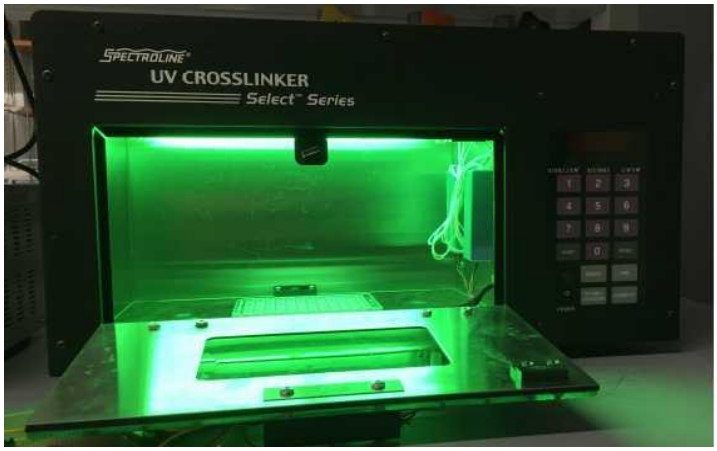

(**a**)

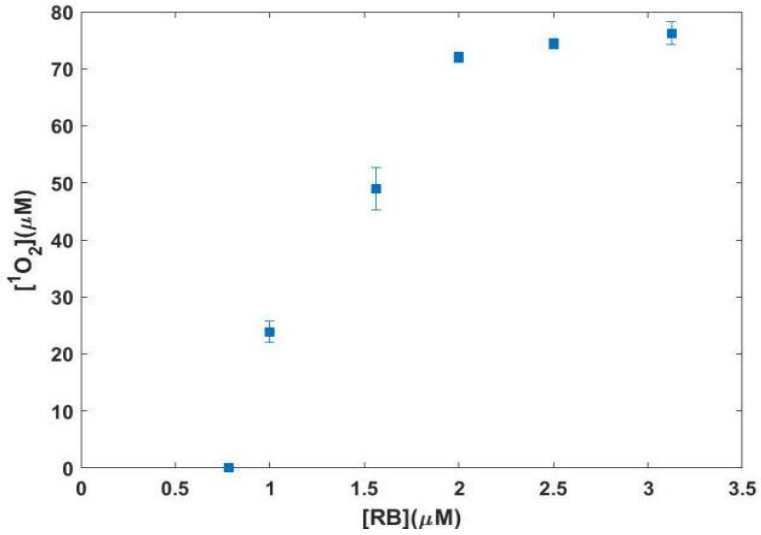

(b)

Figure 1. $^1O_2$ generation via photosensitization of RB in solution followed by detection using an optimized ascorbic acid system (**a**) Green-light illuminator fit with 4 cold cathode green tubes light and operated via an external DC power source. The illuminator provides a constant and uniform source of green light from the top (**b**) Generation of $^1O_2$ as a function of [RB] in solution. There is a linear increase in singlet oxygen generation with [RB] until 2μM beyond where the curve saturates as AA acts as the limiting reagent.

We developed an ACWOP proof-of-concept assay to confirm that our system was capable of detecting non-specific, freely diffusing antibodies in solution via ACWOP. We chose 10μM as the concentration of RB for this assay, as Fig 1b showed that $^1O_2$ generation saturates for [RB]>2μM. Also, for that particular concentration of RB, the limit of detection (LOD) of the generated H_2O_2 in solution is the lowest (Appendix A.2). Sodium azide, commonly used as a preservative, is known to be an inhibitor of $^1O_2$, so azide-free rat IgG was used [21]. The system, consisting of RB and IgG in solution, was placed in the green illuminator to generate $^1O_2$ followed by IgG catalysis via ACWOP to generate H_2O_2 (Fig 2a). The H_2O_2 was detected colorimetrically and we obtained a repeatable non-linear antibody-dependent signal (Fig 2b). Our result corroborates proof-of-concept experiments that were performed by Wentworth et. al. using horse IgG and fluorescent detection, in which they obtained a similar non-linear signal. They hypothesized that the curvature is because of the reduced lifetime of $^1O_2$ in solution due to reaction with the antibody [15]. This demonstration provides the basis for developing a biosensor that can detect antibodies based on the colorimetric H_2O_2 detection signal output produced due to ACWOP.

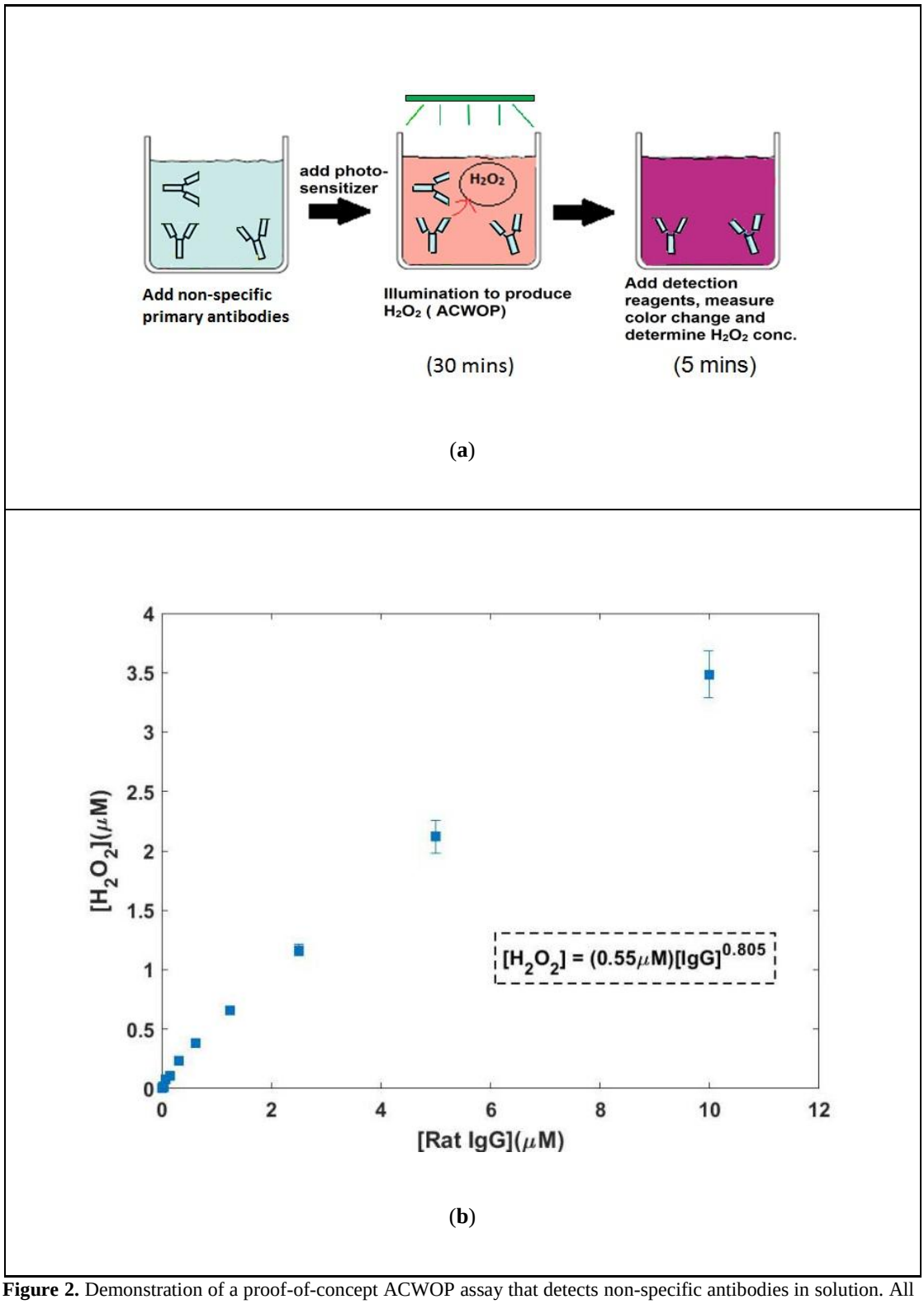

Figure 2. Demonstration of a proof-of-concept ACWOP assay that detects non-specific antibodies in solution. All reagents are freely diffusing in solution. (**a**) Process involved in developing a proof-of-concept assay. Non-specific rat IgG and RB were added to a well, illuminated with green light for 30mins to perform and the generate H_2O_2 was detected via a colorimetric readout (**b**) H_2O_2 generated via ACWOP as a function of non-specific rat IgG freely diffusing in solution. Obtained a repeatable antibody-dependent H_2O_2 generation.

To develop a surface-based ACWOP biosensor that captures primary antibodies and detects them directly, we selected porous silica microparticles as the substrate for functionalizing the photosensitizer and the antigen. We have previously worked with silica surfaces and Welch et. al. have demonstrated an electrochemical ACWOP biosensor using POEGMA brushes functionalized on silicon wafers [22, 23]. APDMES was conjugated to activated-porous silica surfaces via a silanization reaction at elevated temperatures by modifying the protocol used by Wu et.al. [24]. RB was functionalized to the APDMES-silica substrates via an amidation reaction between the carboxylic acid group of the dye and the amine groups on the substrate (Fig 3a) [25]. The absorption spectrum of RB-silica (100µL, 15mg in DPBS) gave a sharp peak at 550nm, the absorption maximum of RB, thereby confirming successful functionalization (Fig 3b).

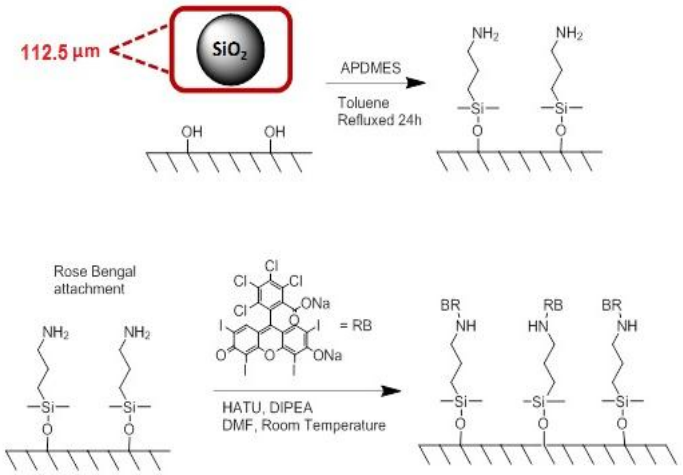

(**a**)

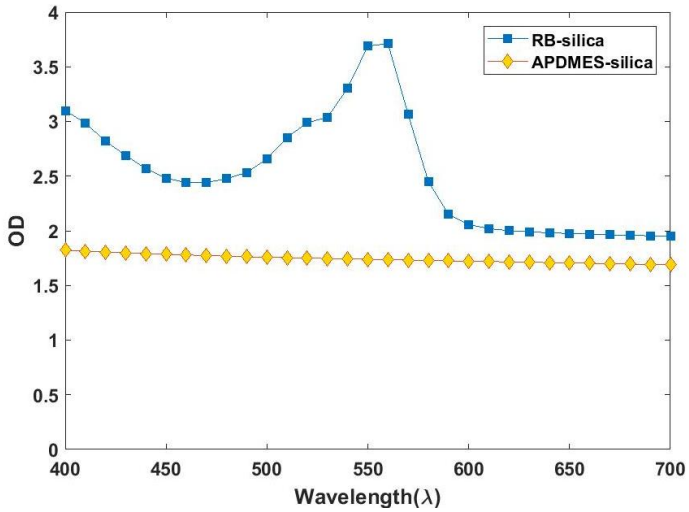

(**b**)

Figure 3. Functionalization of porous silica microparticles with RB (**a**) Chemistry and the process involved in functionalizing 112.5µM porous silica microparticles with RB. Activated silica microparticles are treated with APDMES via a silanization reaction to form APDMES-silica (top). RB is functionalized to APDMES-silica via an amidation reaction to form RB-silica (bottom) (**b**) Confirmation of the presence of RB on RB-silica microparticles using an absorption spectrum. RB-silica shows a peak at 550nm in its absorption spectrum (blue) when compared to APDMES-silica (yellow) confirming successful conjugation of RB.

15mg of RB-silica particles have a total outer surface area of 1.14×10^{-3} that can theoretically bind 2.3×10^{-9} moles of RB (Appendix B.1). This is roughly the same amount of RB that was in solution in the successful proof-of-concept assay. Hence, 15mg of RB-silica particles were illuminated with green light to generate $^1O_2$ on a surface that was detected with ascorbic acid in solution (Fig 4a). Comparison of photosensitization reactions on a surface with the reactions in solution showed a 100-fold higher efficiency of $^1O_2$ generation by RB freely diffusing in solution (Appendix C). These findings are in agreement with Schaap et al. when they compared the efficiency of $^1O_2$ production of free rose bengal with rose bengal immobilized on merrifield polymer and found a 100-fold higher production rate of $^1O_2$ from the free photosensitizer [26]. To further confirm the generation of $^1O_2$ from the RB-silica substrate, we used freely diffusing azide-free rat IgG in solution to catalyze the reaction between the generated $^1O_2$ and water to produce H_2O_2. We obtained repeatable antibody-dependent H_2O_2 generation, thereby validating the RB-silica microparticles as reliable sources of $^1O_2$ (Fig 4b).

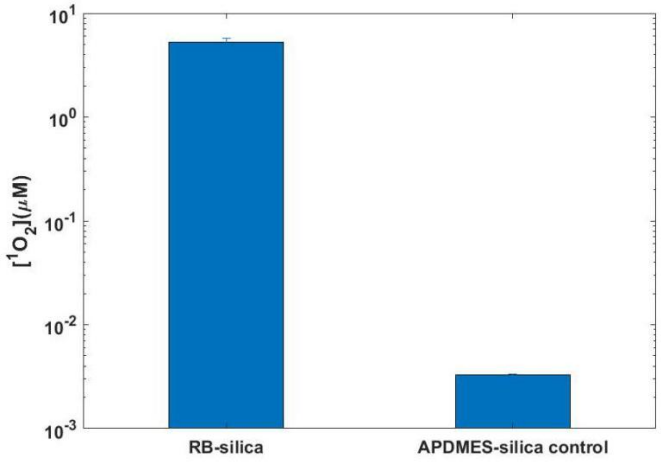

(**a**)

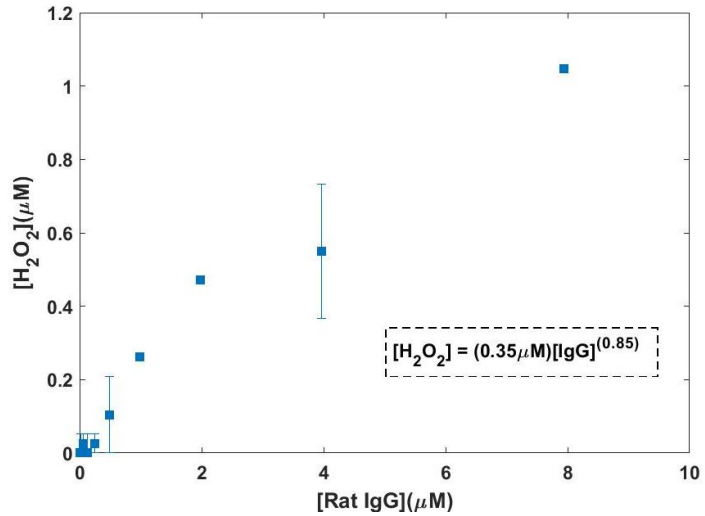

(**b**)

Figure 4. $^1O_2$ generation via photosensitization of RB on a surface followed by detection using two different methods (**a**) Ascorbic acid detection. 15mg of RB-silica microparticles generated $^1O_2$ on illumination with green light. APDMES-silica microparticles (control) that have no RB functionalized to the surface produced no $^1O_2$ (**b**) Freely diffusing non-specific antibodies in solution via ACWOP. $^1O_2$ generated by 15mg RB-silica microparticles reacted with water in the presence of rat IgG to generate H_2O_2. Obtained a repeatable antibody-dependent signal confirming generation of $^1O_2$ from RB surfaces.

We utilize 2, 4-DNP as a model antigen that is bound by anti-DNP antibodies from several species and classes for initial development of our ACWOP biosensor [22]. DNP ε-amino n-caproic acid was functionalized to the APDMES-silica microparticles in a manner similar to that for RB. An amidation reaction occurs between the carboxylic acid group of DNP and the free amine on the APDMES-silica microparticles.

We confirmed the capture of anti-DNP primary IgG on DNP-silica microparticles using secondary fluorophore-tagged antibodies. 30mg of DNP-silica microparticles were used as that provided 71 times more surface area than the bottom of a well in an ELISA plate, thereby providing more binding sites for antibody capture (Appendix B.2). The process involved incubation of the DNP-silica microparticles with primary goat anti-DNP IgG, incubation with secondary donkey anti-goat IgG and fluorescence intensity measurement with a plate reader (Fig 5a). We observed an increase in the fluorescence readout from the secondary antibody with increasing primary antibody concentration used for incubation (Fig 5b). This confirms primary-antibody concentration dependent capture on DNP-silica particles that saturates at higher IgG concentrations possibly due to limited number of binding sites.

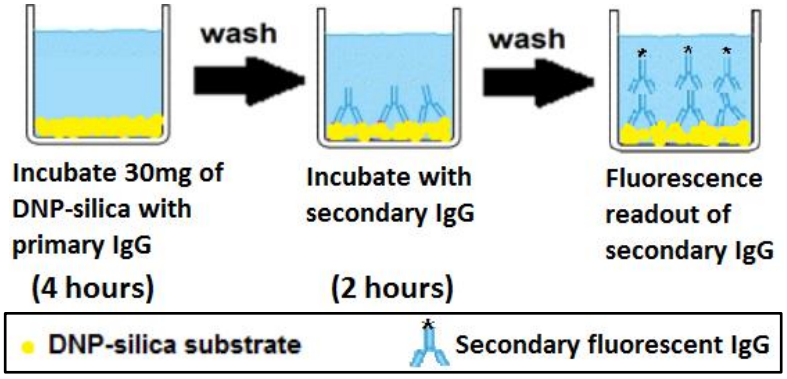

(**a**)

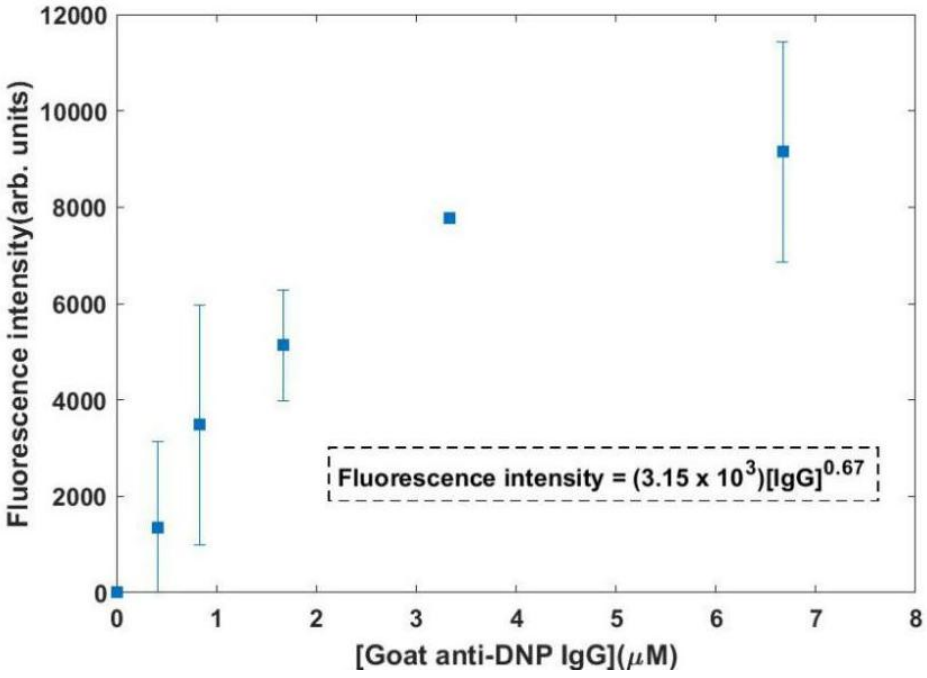

(**b**)

Figure 5. Confirmation of capture of primary anti-DNP antibodies on DNP-silica microparticles using fluorophore-tagged secondary antibodies (**a**) Process involved in developing a secondary readout from captured primary antibodies. Primary antibody: goat anti-DNP IgG, secondary antibody: AlexaFluor 568 donkey anti-goat IgG. (**b**) Fluorescence readout from secondary antibody bound to captured primary antibodies on DNP-silica. Obtained a repeatable primary-antibody dependent signal confirming successful capture.

The generation of ACWOP signal from the surface-based biosensor involved the following process: (a) capture of primary antibodies on DNP-silica microparticles, (b) generation of $^1O_2$ from RB-silica microparticles and (c) antibody catalysis to generate H_2O_2 that is detected colorimetrically (Fig 6a). DNP-silica microparticles were incubated with mouse anti-DNP IgG using the validated protocol used previously. Because the lifetime of $^1O_2$ in aqueous solutions is in the range of 1-10μs, which corresponds to a mean square diffusion distance of less than 0.5μm (diffusion coefficient of O_2: 2 x 10^{-5} cm^2/sec), the DNP-silica and RB-silica microparticles were mixed well together to ensure close proximity of the $^1O_2$ to the antibody [27]. The system was illuminated with green light to generate $^1O_2$ that reacted with water in the presence of the captured antibodies to produce H_2O_2. We obtained a captured primary antibody-dependent H_2O_2 production (Fig 6b). A negative control of normal-mouse IgG was performed using the same protocol to determine non-specific binding of IgG to silica surfaces. On comparison the H_2O_2 generation from the specific DNP-captured antibody was higher than the control. The curve for the ACWOP readout of primary anti-DNP antibodies exhibits a curvature with decreasing slope at higher concentrations of IgG, either because of saturation of primary antibody binding sites as seen in the previous section or because of the short lifetime of $^1O_2$ due to consumption as postulated by Wentworth in the proof of concept assay [15].

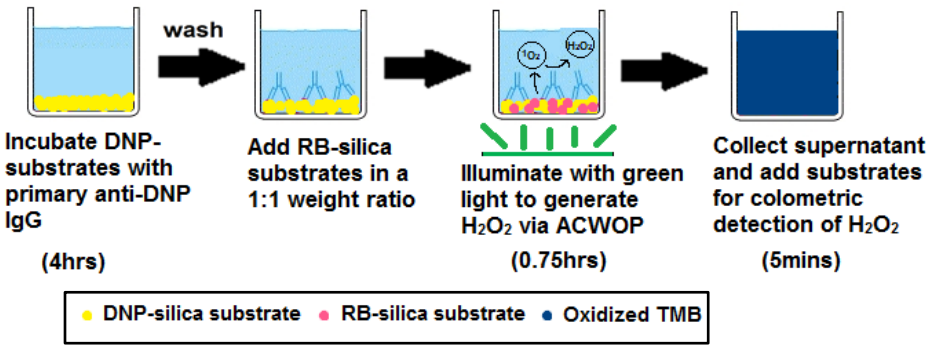

(**a**)

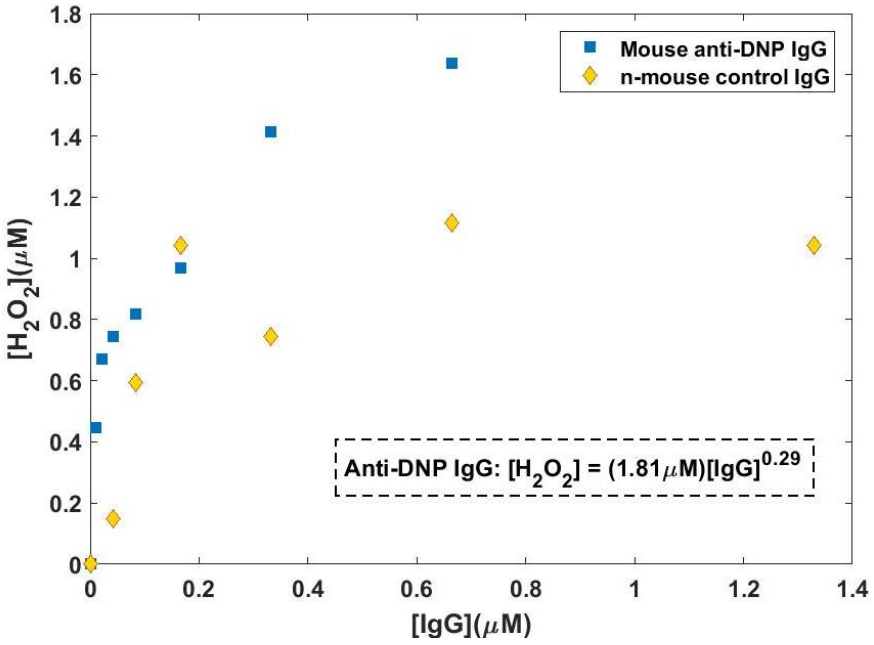

(b)

Figure 6. Demonstration of a novel surface-based ACWOP biosensor that can directly detect captured primary antibodies and generate a colorimetric readout (**a**) Process involved in capture and detection of anti-DNP primary antibodies using the ACWOP biosensor. Mouse anti-DNP IgG were captured on DNP-silica. $^1O_2$ generated by RB-silica reacts with water in presence of captured antibodies to generate H_2O_2 which is detected via a colorimetric readout (**b**) Obtained a primary antibody-dependent H_2O_2 generation (blue). A negative control with n-mouse IgG showed non-specific binding of IgG to silica substrates (yellow). The non-specific capture (yellow) occurred to a lesser extent than the specific DNP capture (blue)

5. Conclusions

In summary, we have developed a novel silica-microparticle based biosensor that directly detects captured primary antibodies via the ACWOP and generates an antibody-dependent colorimetric signal. By eliminating the use of secondary antibodies that are specific to species, our ACWOP biosensor is capable of directly detecting antibodies from any species. The sensor improves testing time by eliminating the 2-hour incubation step required for binding secondary reagents in traditional ELISA kits. We have used relatively inexpensive substrates and reagents, which, coupled with the elimination of expensive, specially prepared secondary reagents, decreases the overall cost of our sensor. In this way, the surface-based sensor provides a universal platform for direct antibody detection in a species-independent manner. Future studies involve modification of this platform into a lateral flow test format for point-of-care monitoring of infectious diseases in multiple hosts via ACWOP.

Author Contributions: Conceptualization, Brian Kirby and Christopher Ober.; Methodology, Pranav Sundaram; Validation, Andrew Sanchez; Formal Analysis, Pranav Sundaram; Investigation, Pranav Sundaram and Andrew Sanchez; Resources, Roselynn Cordero, Wei-Liang Chen and Brian Kirby; Data Curation, Pranav Sundaram.; Writing-Original Draft Preparation, Pranav Sundaram; Writing-Review & Editing, Brian Kirby, Christopher Ober and Andrew Sanchez; Visualization, Pranav Sundaram, Andrew Sanchez and Roselynn Cordero; Supervision, Brian Kirby and Christopher Ober; Project Administration, Pranav Sundaram and Andrew Sanchez; Funding Acquisition, Brian Kirby and Christopher Ober

Funding: This research was funded by the National Science Foundation, grant number: 1706518.

Conflicts of Interest: The authors declare no conflict of interest. The funders had no role in the design of the study; in the collection, analyses, or interpretation of data; in the writing of the manuscript, and in the decision to publish the results.

Appendix A

A.1 Development and optimization of a hydrogen peroxide colorimetric detection system

[HRP] optimization:

HRP (100µL, 11µM) was serially diluted in DPBS (pH 7.4, 100µL) with a dilution factor of 1/2 in 11 wells of a clear 96-well microplate. A well containing DPBS (pH 7.4, 100µL) was used as the negative control. H_2O_2 (100µL, 20µM) and TMB (100µL, 1.04mM) was added to each well. The plate was covered with aluminium foil and incubated for 5 minutes. The absorbance intensity at 650nm was measured using a plate reader for all the wells. The above experiment was performed in triplicate and each data point is reported as the mean ± S.E.M.

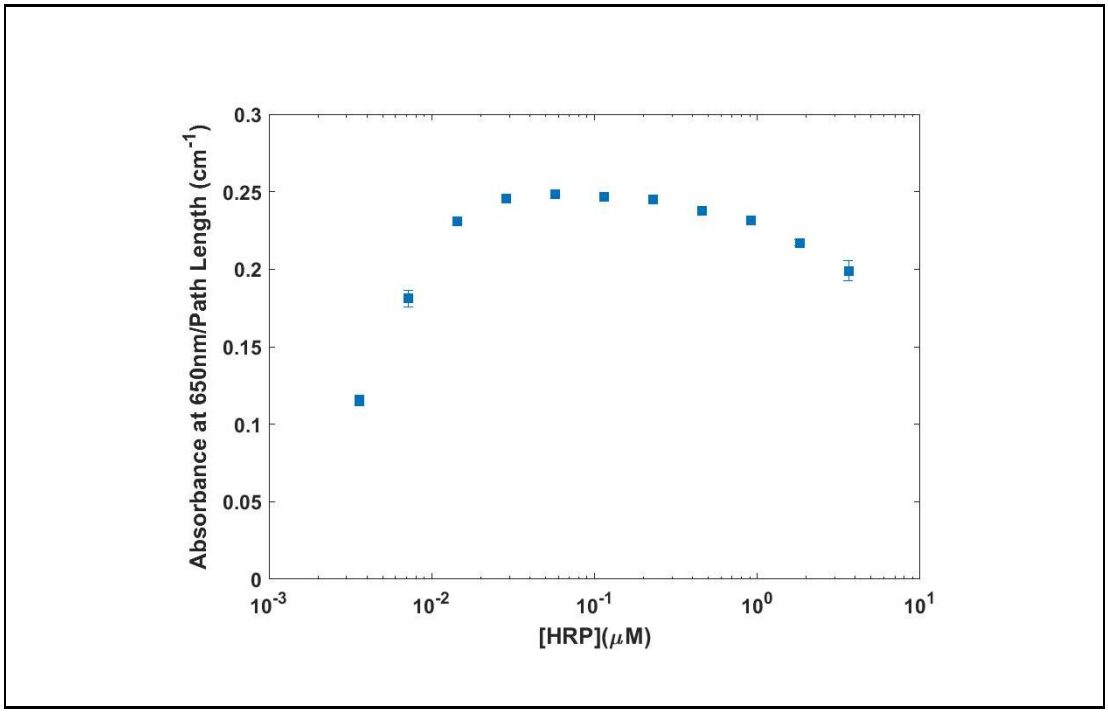

Figure A1. Optimization of [HRP] to obtain maximum colorimetric H_2O_2 detection signal. [H_2O_2] = 20µM, [TMB] = 1.04mM and time = 5 minutes.

The optimum [HRP] was chosen to be **0.171µM**.

[TMB] optimization:

TMB (100µL, 1.04mM) was serially diluted in DPBS (pH 7.4, 100µL) with a dilution factor of 1/2 in 11 wells of a clear 96-well microplate. A well containing DPBS (pH 7.4, 100µL) was used as the negative control. H_2O_2 (100µL, 44µM) and HRP (20µL, 0.171µM) was added to each well. The plate was covered with aluminium foil and incubated for 5 minutes. The absorbance intensity at 650nm was measured using a plate reader for all the wells. The above experiment was performed in triplicate and each data point is reported as the mean $\pm$ S.E.M.

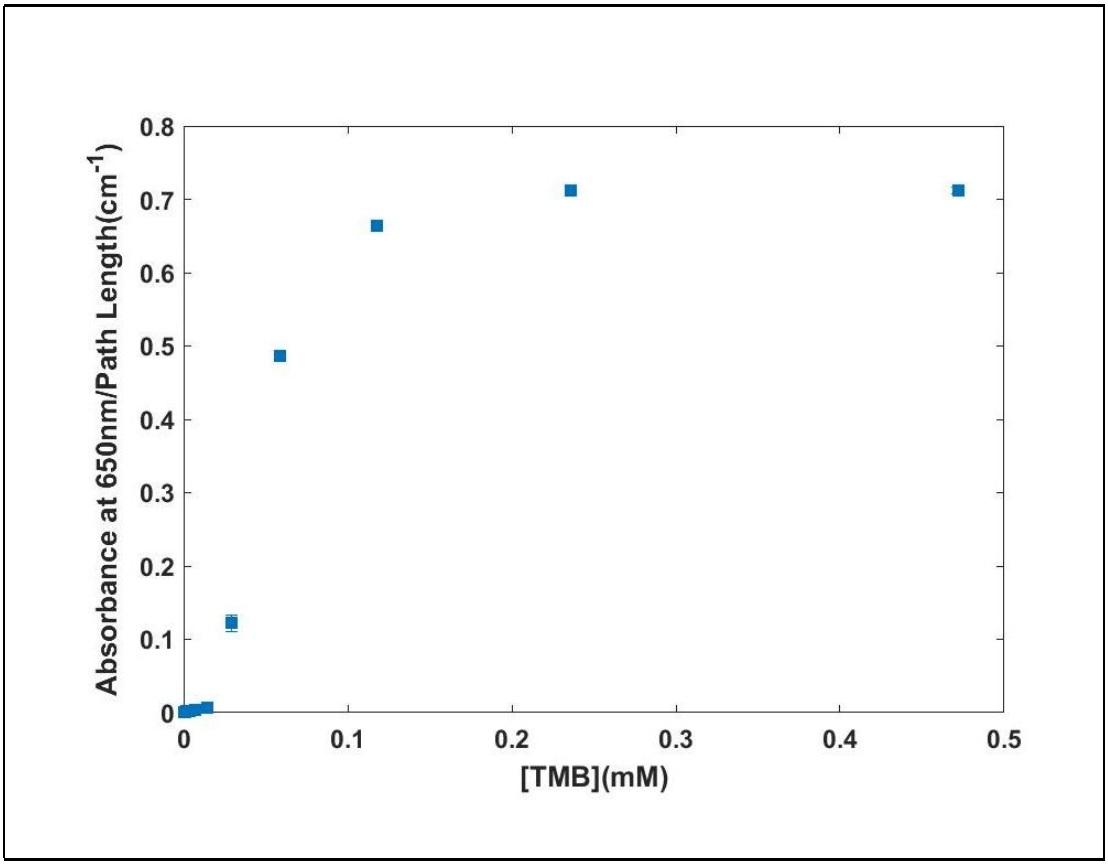

Figure A2. Optimization of [TMB] to obtain maximum colorimetric H_2O_2 detection signal. [H_2O_2] = 44µM, [HRP] = 0.171mM and time = 5 minutes.

The blue color change takes place when $[H_2O_2] \leq [TMB]$ and at equimolar concentration the color is most intense. Based on this observation, an optimum [TMB] of **1.04mM** was chosen as the stock solution [18].

Hydrogen peroxide standard curve for proof-of-concept assay:

H_2O_2 was detected by the oxidative color change of TMB in the presence of HRP. H_2O_2 (100µL, 64µM stock) was serially diluted in DPBS (pH 7.4, 100µL) with a dilution factor of 1/2 in 11 wells of a clear 96-well microplate. A well containing DPBS (pH 7.4, 100µL) was used as the negative control. RB (100µL, 0.01mM stock), HRP (20µL, 0.171µM stock) and TMB (100µL, 1.04mM stock) were added to all 12 wells. The plate was covered with aluminium foil and incubated for 5 minutes. The absorbance intensity at 650nm was measured using a plate reader for all the wells. The above experiment was performed in triplicate and each data point is reported as the mean $\pm$ S.E.M.

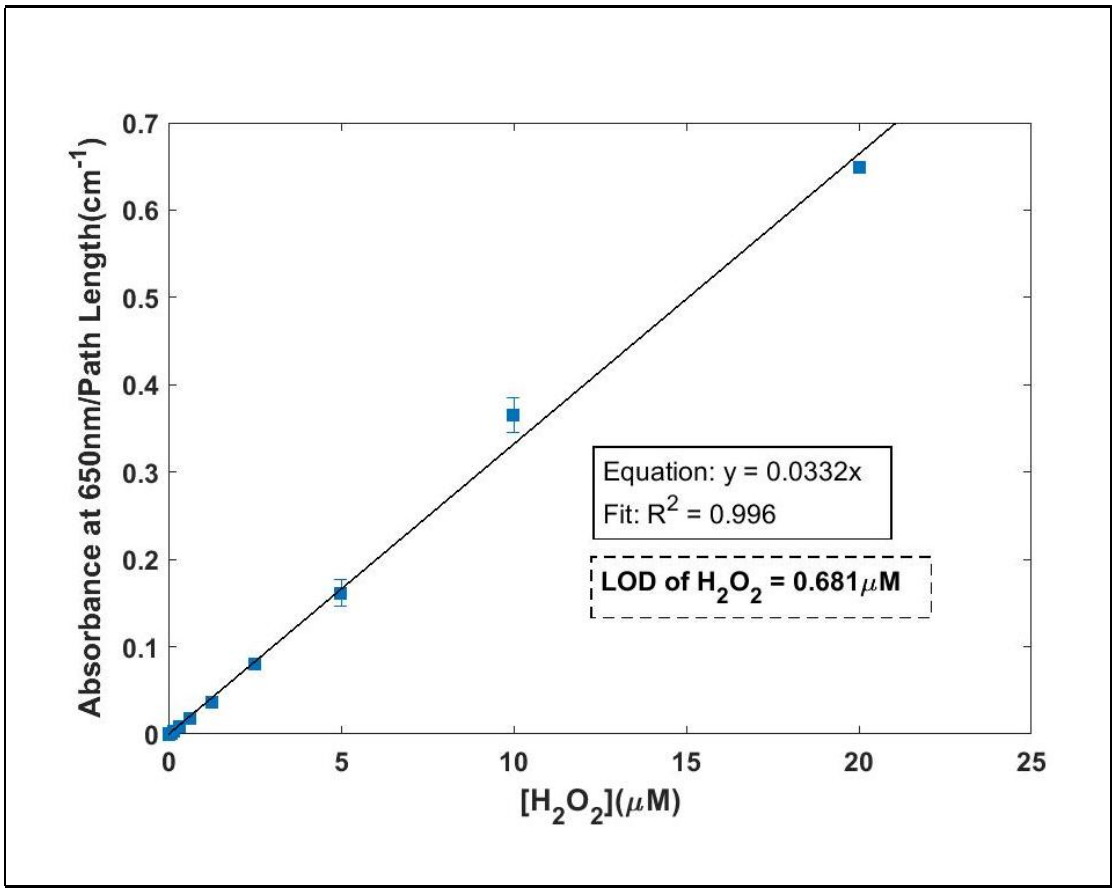

Figure A3. H_2O_2 standard curve for the proof-of-concept assay. Colorimetric signal obtained from the plate reader is converted to [H_2O_2] based on the relation provided in the inset. [HRP] = 0.171µM, [TMB] = 1.04mM, [RB] = 0.01mM and time = 5 minutes.

Hydrogen peroxide standard curve for RB-silica microparticle based experiments:

H_2O_2 was detected by the oxidative color change of TMB in the presence of HRP. H_2O_2 (100µL, 64µM stock) was serially diluted in DPBS (pH 7.4, 100µL) with a dilution factor of 1/2 in 11 wells of a clear 96-well microplate. A well containing DPBS (pH 7.4, 100µL) was used as the negative control. HRP (20µL, 0.171µM stock) and TMB (100µL, 1.04mM stock) were added to all 12 wells. The plate was covered with aluminium foil and incubated for 5 minutes. The absorbance intensity at 650nm was measured using a plate reader for all the wells. The above experiment was performed in triplicate and each data point is reported as the mean $\pm$ S.E.M.

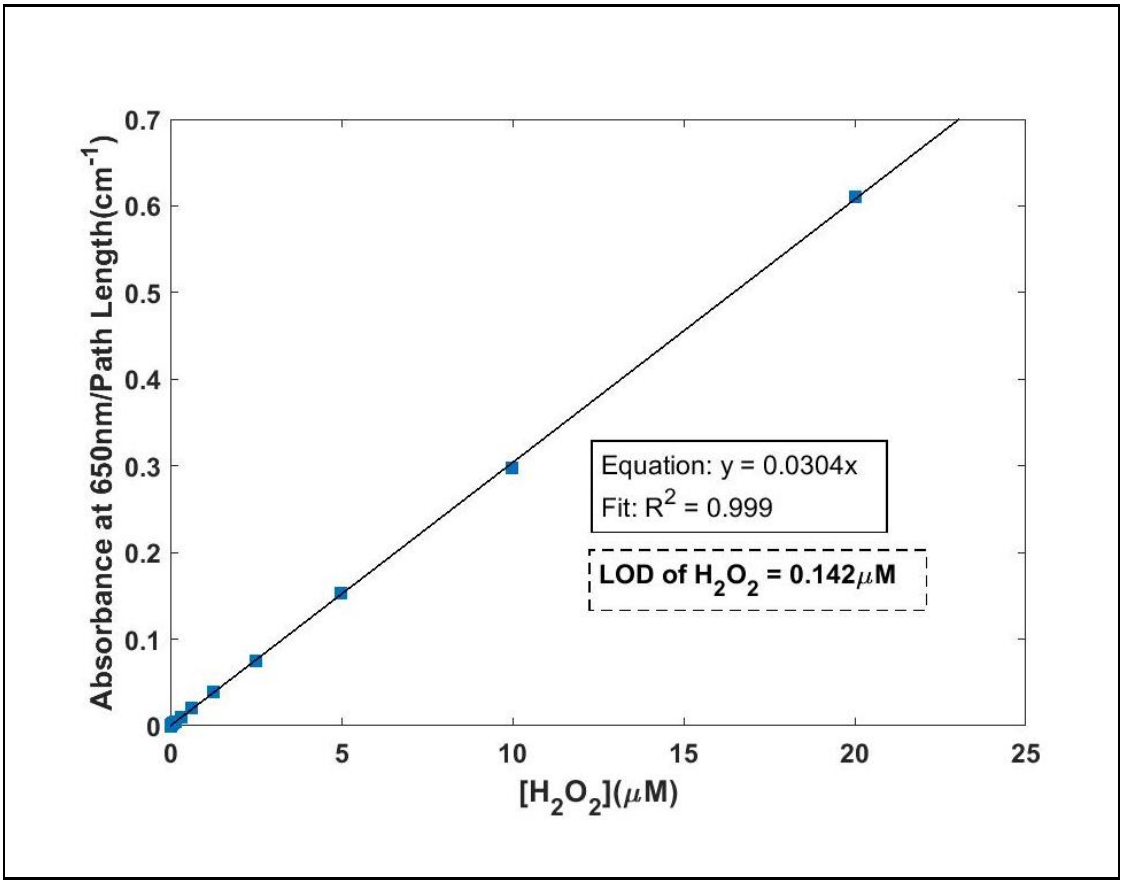

Figure A4. H_2O_2 standard curve for surface-based sensor experiments. Colorimetric signal obtained from the plate reader is converted to [H_2O_2] based on the relation provided in the inset. [HRP] = 0.171µM, [TMB] = 1.04mM and time = 5 minutes.

A.2 Limit of detection of hydrogen peroxide in different Rose Bengal concentrations in solution

H_2O_2 (100µL, 64µM stock) was serially diluted in DPBS (pH 7.4, 100µL) with a dilution factor of 1/2 in 11 wells of a clear 96-well microplate. A well containing DPBS (pH 7.4, 100µL) was used as the negative control. RB (100µL, 0.01M stock), HRP (20µL, 0.171µM stock) and TMB (100µL, 1.04mM stock) were added to all 12 wells. The plate was covered with aluminium foil and incubated for 5 minutes. The absorbance intensity at 650nm was measured using a plate reader for all the wells. 4

other RB stock conditions - 1mM, 0.1mM, 0.01mM and 1µM were tested following the same protocol as above. All experiments were performed in triplicate and each data point is reported as the mean ± S.E.M.

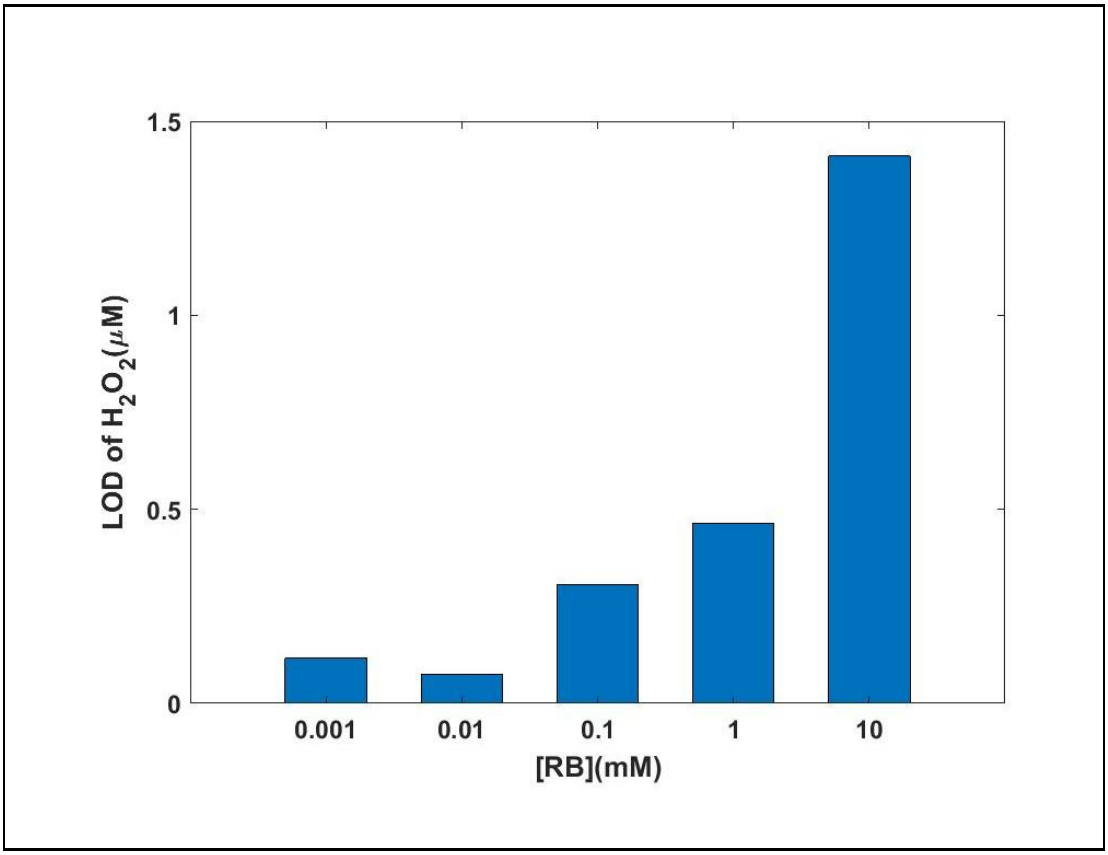

Figure A5. Analysis of LOD of H_2O_2 for different [RB] in solution. RB = 0.01mM provided the best(lowest) LOD and hence was chosen as the RB concentration in the ACWOP proof-of-concept assay.

RB=0.01mM gave the lowest limit of detection and was chosen as the optimum [RB] for the proof-of-concept ACWOP assay.

Appendix B

B.1 Calculation of number of moles of RB present on 15mg of RB-silica microparticles

Bulk density of silica gel = 700kg/m^3

Hence 15mg of silica gel has a total volume = 2.142 x 10^{-8} m^3

From the manufacturer's specification, porous silica gel corresponds to -100+200 mesh which means the size of a particle lies between 75 to 150 µm.

Assuming an average of 112.5µm, the radius of a single particle = R = 56.25µm.

$$\text{Volume of a particle} = \frac{4 \times \pi \times R^3}{3} = 7.45 \times 10^{-13}\ m^3$$

Number of silica microparticles in 15mg = Total volume/Volume of a particle = 28752 particles

$$\text{Outer surface area of one particle} = 4 \times \pi \times R^2 = 3.97 \times 10^{-8}\ m^2$$

Total outer surface area of all particles =

Number of particles x Outer surface area of a particle = 1.14 x 10^{-3} m^2

Molar volume of Rose Bengal = 338 x 10^{-6} m^3

Volume of single RB molecule = Molar volume/N_A(Avagadro number) = 5.611 x 10^{-28} m^3

Radius of a single RB molecule = $\sqrt[3]{\frac{\text{Volume of a single molecule x 3}}{4 \text{ x } \pi}}$ = 0.511 nm

Cross sectional area of a single molecule = π x R^2 = 8.22 x 10^{-19} m^2

Total number of RB molecules that can fit on the silica surface =

Total outer surface area / Cross sectional area of an RB molecule = 1.38 x 10^{15} molecules.

Total moles of RB that can be functionalized on the outer surface of 15mg of silica microparticles = Total number of RB molecules/N_A = **2.3 x 10^{-9} moles**

B.2 Comparison of Total Surface Area(TSA) provided by 30mg DNP-silica particles with the TSA of the bottom of a well in a 96-well ELISA microplate:

Bulk density of silica gel = 700kg/m^3

Hence 30mg of silica gel has a total volume = 4.285 x 10^{-8} m^3

From the manufacturer's specification, porous silica gel corresponds to -100+200 mesh. This means the size of a particle lies between 75 to 150 µm.

Assuming an average of 112.5µm, the radius of a single particle = R = 56.25µm.

Volume of a particle = $\frac{4 \text{ x } \pi \text{ x } R^3}{3}$ = 7.45 x 10^{-13} m^3

Number of silica microparticles in 30mg = Total volume/Volume of a particle = 57517 particles

Outer surface area of one particle = $4 \times \pi \times R^2 = 3.97 \times 10^{-8}\ m^2$

Total outer surface area of all particles = Number of particles x Outer surface area of a particle = $2.28 \times 10^{-3}\ m^2$

Radius of the bottom of a F-bottom well from greiner bio-one, $R = 3.195 \times 10^{-3}$ m

Total surface area of the bottom of the well = $\pi \times R^2 = 3.2 \times 10^{-5}\ m^2$

Ratio of Surface areas = Total Surface area of 30mg DNP-silica particles/Total surface area of the bottom of an ELISA well = **71**

Appendix C

Comparison of the singlet oxygen generation efficiency between Rose Bengal freely diffusing in solution and RB functionalized to silica microparticles

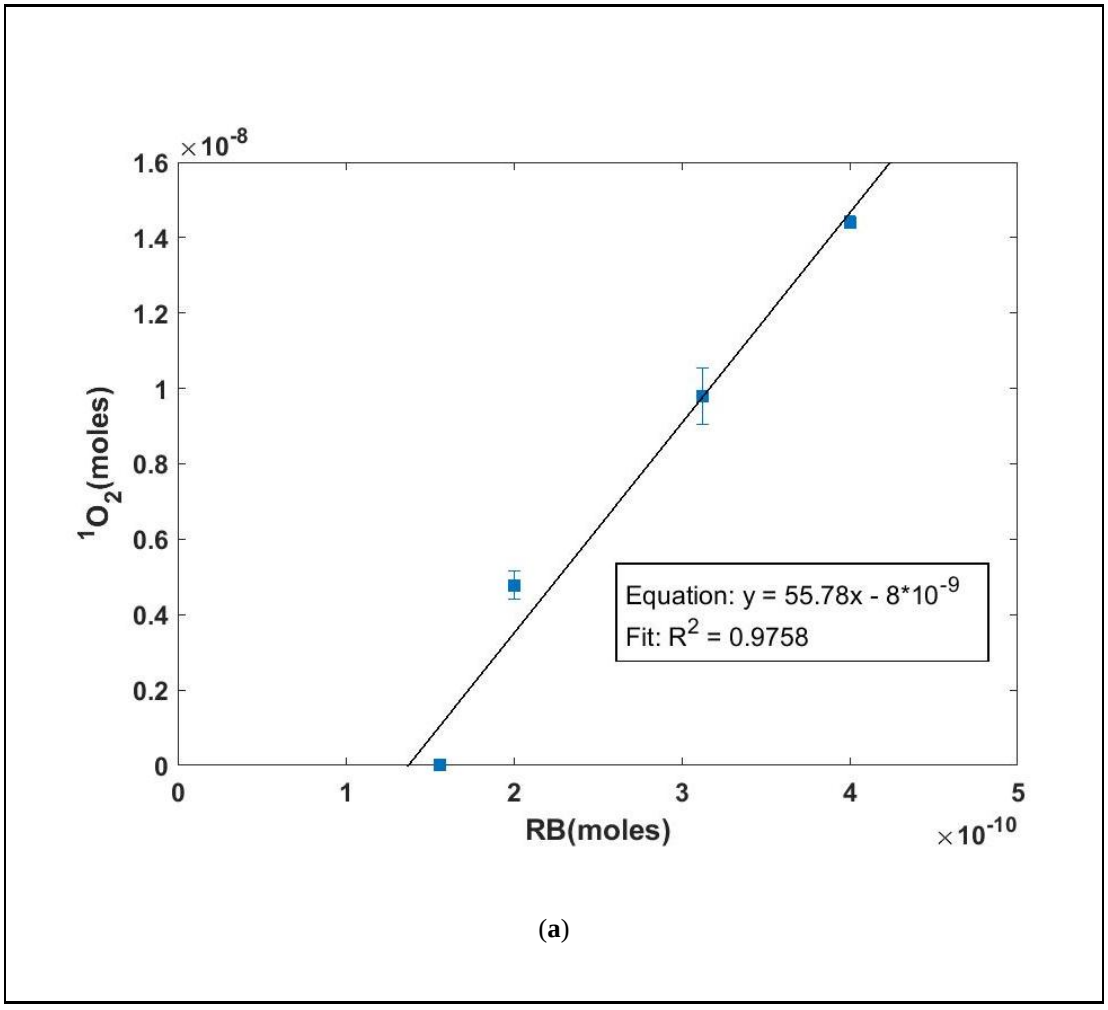

(**a**)

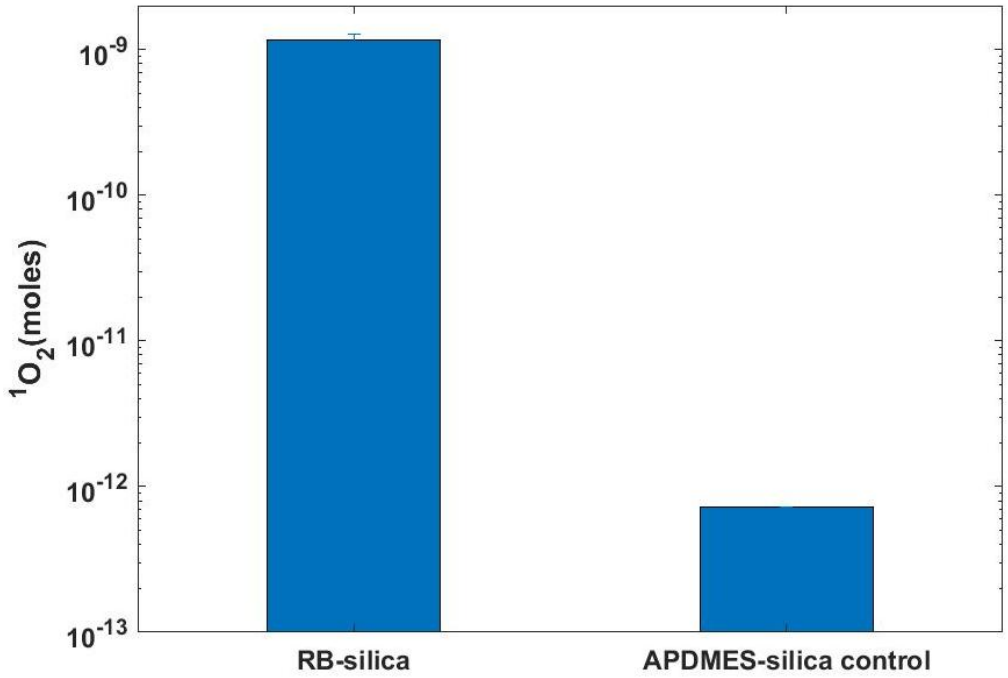

(**b**)

Figure C. Comparison between photosensitization reactions in solution and on a surface (**a**) Analysis of number of moles of $^1O_2$ generated per mole of RB in solution (**b**) Analysis of number of moles of $^1O_2$ generated per moles of RB on a surface

Rose Bengal in solution: From Fig C(a), $^1O_2$ moles generated/RB moles in solution = 55.78 Therefore, 1 mole of RB in solution generates 55.78 moles of $^1O_2$ in 30 minutes. Rose Bengal functionalized to silica microparticles: From Appendix B.1, moles of RB on 15mg silica particles = 2.3 x 10^{-9} moles.	(1)

From Fig C, $^1O_2$ moles generated from 15mg RB-silica = 1.15×10^{-9} moles $^1O_2$ moles generated/RB moles on surface = 0.5 Therefore 1 mole of RB on the surface generates 0.5 moles of $^1O_2$ in 30 minutes. Ratio of (1)/(2) = 55.78/0.5 = **111.56** RB in solution generates 111.56 more moles of $^1O_2$ than RB on surface. Hence RB freely diffusing in solution is 100 times more efficient in generating $^1O_2$ than RB functionalized on silica particles.	(2)

References

1. Bean et. al.; Studying immunity to zoonotic diseases in the natural host - keeping it real; Nat Rev Immunol.; 2013 Dec; 13(12):851-61. doi: 10.1038/nri35.

2. Russell CJ et al.; Influenza Hemagglutinin Protein Stability, Activation, and Pandemic Risk.; Trends Microbiol.; 2018 Apr 19.; pii: S0966-842X(18)30068-4. doi: 10.1016/j.tim.2018.03.005.

3. Potter, C. W.; A history of influenza.; J. Appl. Microbiol.; 2001; 91, 572.

4. Sturm-Ramirez, K. M. et.al.; Reemerging H5N1 influenza viruses in Hong Kong in 2002 are highly pathogenic to ducks.; J. Virol.; 2004; 78, 4892.

5. Dye C.; After 2015: infectious diseases in a new era of health and development.; Philosophical Transactions of the Royal Society B: Biological Sciences.; 2014; 369(1645):20130426. doi:10.1098/rstb.2013.0426.

6. Simonds, Anita K.; Influenza News from the Frontline: What's Happening?; ERJ Open Research 4.1; 2018; 00020–2018. PMC. Web. 5 June 2018.

7. Lashley et. al.; Factors Contributing to the Occurrence of Emerging Infectious Diseases; Biological Research For Nursing, Vol 4, Issue 4, pp. 258 – 267.

8. Velumani, S.; Ho, H.-T.; He, F.; Musthaq, S.; Prabakaran, M.; Kwang, J.; PLoS One 2011, 6, e20737.

9. Washington JA.; Principles of Diagnosis. In: Baron S, editor.; Medical Microbiology. 4th edition. Galveston (TX): University of Texas Medical Branch at Galveston; 1996. Chapter 10.

10. Yolken RH.; Enzyme-linked immunosorbent assay (ELISA): a practical tool for rapid diagnosis of viruses and other infectious agents.; The Yale Journal of Biology and Medicine.; 1980; 53(1):85-92.

11. Stricker RB, Johnson L.; Let's tackle the testing; BMJ : British Medical Journal.; 2007; 335(7628):1008.

12. Manning, Colleen F., Angeliki M. Bundros, and James S. Trimmer.; Benefits and Pitfalls of Secondary Antibodies: Why Choosing the Right Secondary Is of Primary Importance.; Ed. Joy Sturtevant.; PLoS ONE 7.6 (2012): e38313. PMC. Web. 5 June 2018.

13. Voskuil J.; Commercial antibodies and their validation; Version 1.; F1000Res.; 2014; 3: 232.

14. Wentworth, P.; Jones, L. H.; Wentworth, A. D.; Zhu, X. Y.; Larsen, N. A.; Wilson, I. A.; Xu, X.; Goddard, W. A.; Janda, K. D.; Eschenmoser, A.; Lerner, R. A.; Science; 2001; 293, 1806.

15. Wentworth A D, Jones L H, Wentworth P, Janda K D, Lerner R A(2000); Proc Natl Acad Sci USA; 97:10930–10935. pmid:11005865.

16. Zhu, X. Y.; Wentworth, P.; Wentworth, A. D.; Eschenmoser, A.; Lerner, R. A.; Wilson, I. A.; Proc. Natl. Acad. Sci. U.S.A.; 2004; 101,2247.

17. Datta, D.; Vaidehi, N.; Xu, X.; Goddard, W. A.; Proc. Natl. Acad. Sci.; U.S.A.; 2002; 99 (5) 2636– 2641.

18. Josephy PD, et. al.; The horseradish peroxidase-catalyzed oxidation of 3,5,3',5'-tetramethylbenzidine. Free radical and charge-transfer complex intermediates.; J Biol Chem.; 1982 Apr 10; 257(7):3669-75.

19. M.C. DeRosa, R.J. Crutchley; Photosensitized singlet oxygen and its applications; Coordination Chemistry Reviews; 233/234 (2002) 351/371.

20. Kramarenko GG, Hummel SG, Martin SM, Buettner GR; Ascorbate Reacts with Singlet Oxygen to Produce Hydrogen Peroxide; Photochem Photobiol.; 2006; 82(6): 1634–1637.doi: 10.1562/2006-01-12-RN-774.

21. Bancirova, M. (2011); Sodium azide as a specific quencher of singlet oxygen during chemiluminescent detection by luminol and Cypridina luciferin analogues.; Luminescence; 26: 685-688. doi:10.1002/bio.1296.

22. M. Elizabeth Welch, Nicole L. Ritzert, Hongjun Chen, Norah L. Smith, Michele E. Tague, Youyong Xu, Barbara A. Baird, Héctor D. Abruña, and Christopher K. Ober; Journal of the American Chemical Society; 2014; 136 (5), 1879-1883. DOI: 10.1021/ja409598c.

23. Wei-Liang Chen, Roselynn Cordero, Hai Tran, and Christopher K. Ober; Macromolecules; 2017; 50 (11), 4089-4113. DOI: 10.1021/acs.macromol.7b00450

24. Wu N. et. al.; A novel surface molecularly imprinted polymer as the solid-phase extraction adsorbent for the selective determination of ampicillin sodium in milk and blood samples; J Pharm Anal.; 2016 Jun; 6(3):157-164. doi: 10.1016/j.jpha.2016.01.004.

25. Guo, Yanyan, Snezna Rogelj, and Peng Zhang.; Rose Bengal-Decorated Silica Nanoparticles as Photosensitizers for Inactivation of Gram-Positive Bacteria.; Nanotechnology 21.6 (2010): 065102. PMC. Web. 5 June 2018.

26. Schaap, A. P., A. L. Thayer, G. L. Faler, K. Coda and T. Kimura (1974) J. Am. Chem. Soc. 96, 4025-6.

27. Merkel, P. B.; Kearns, D. R.; Nilsson, R.; Deuterium effects on singlet oxygen lifetimes in solutions. New test of singlet oxygen reactions; J. Am. Chem. Soc.; 1972; 94, 1030.

Supplementary Information

1. Absorption spectrum of RB in solution:

RB (100µL, 0.01mM) in DPBS (pH 7.4, 1x) was taken in a well and the absorbance spectrum was performed using a plate reader. The spectrum showed that the photosensitizer has an absorption maximum at 550nm i.e. green light.

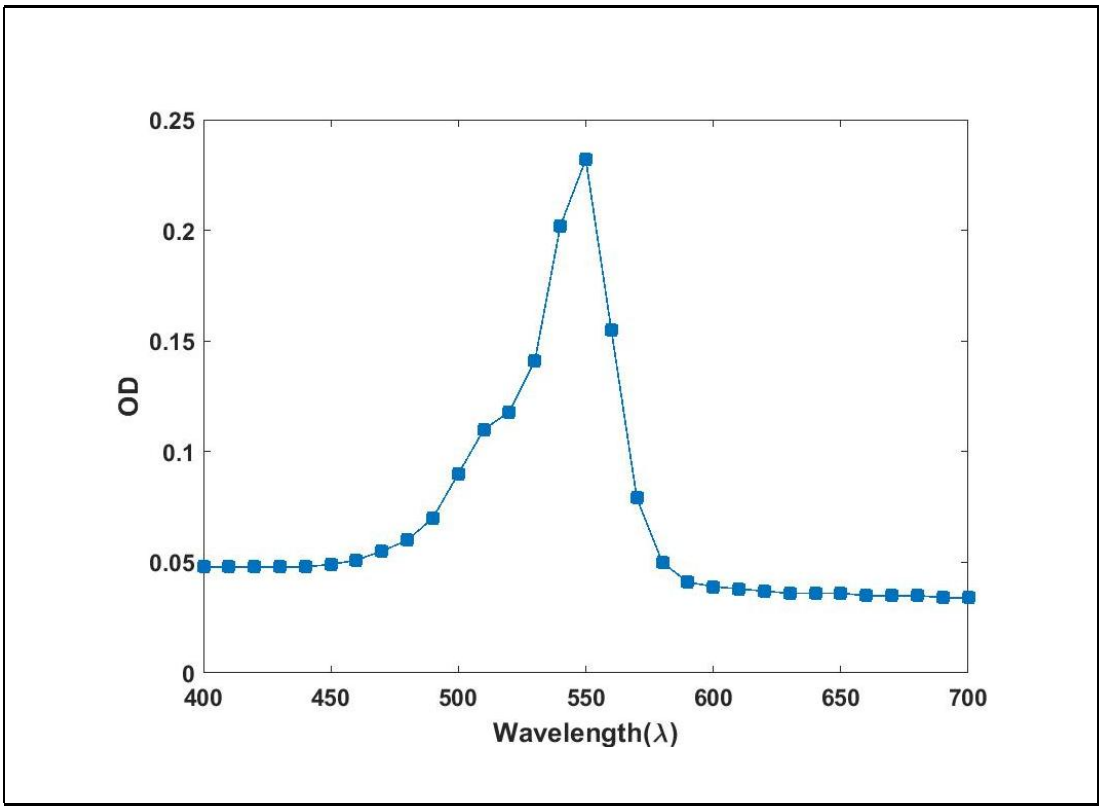

Figure S1. Absorption spectrum of 0.01mM RB in solution. Absorption maximum occurs at 550nm i.e. green light.

2. pH as a function of Ascorbic Acid concentration:

Ascorbic Acid (5mL, 0.07M) was serially diluted in 1x DPBS (phosphate 10mM/sodium chloride 160mM, pH 7.4, 5mL) with a dilution factor of ½ in 11 scintillation vials. A control of 1x DPBS (pH 7.4, 5mL) was taken in a separate vial. The pH was measured using a Mettler Toledo 7 pH/conductivity meter.

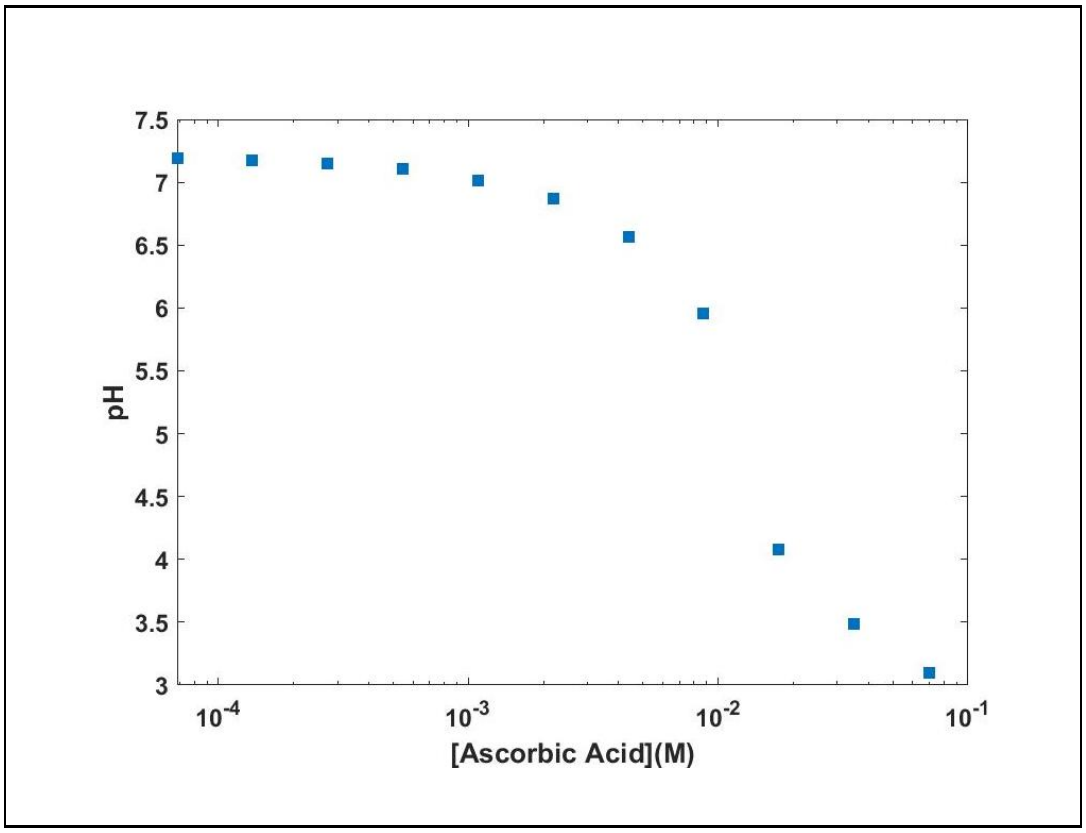

Figure S2. pH of ascorbic acid dissolved in DPBS as a function of [ascorbic acid]. For AA>10mM (buffering capacity of DPBS), the pH drops steeply.

For AA>10mM, there was a sharp drop in pH below 7.4 because the buffering capacity of 1x DPBS was 10mM.

3. Optimization of Ascorbic Acid for various concentrations of Rose Bengal in solution:

Ascorbic Acid (100µL, 10mM stock) was serially diluted in DPBS (pH 7.4, 100µL) with a dilution factor of 1/2 in 11 wells of a clear 96-well microplate. A well containing DPBS (pH 7.4, 100µL) was used as the negative control. RB (100µL, 0.01M stock) was added to each well. The plate was placed in the green-light illuminator and illuminated from the top for 60 minutes. HRP (20µL, 0.171uM stock) and TMB (100µL, 1.04mM stock) were added to each well. The plate was covered with aluminium foil and incubated for 5 minutes. The absorbance intensity at 650nm was measured for each well in a plate reader. 4 other RB stock conditions - 1mM, 0.1mM, 0.01mM and 1µM were tested for following the same protocol as above. All of the experiments for different RB conditions were performed in triplicate and each data point is reported as the mean $\pm$ S.E.M. The absorbance intensity at 650nm was converted to $[H_2O_2]$ using the H_2O_2 standard curve.

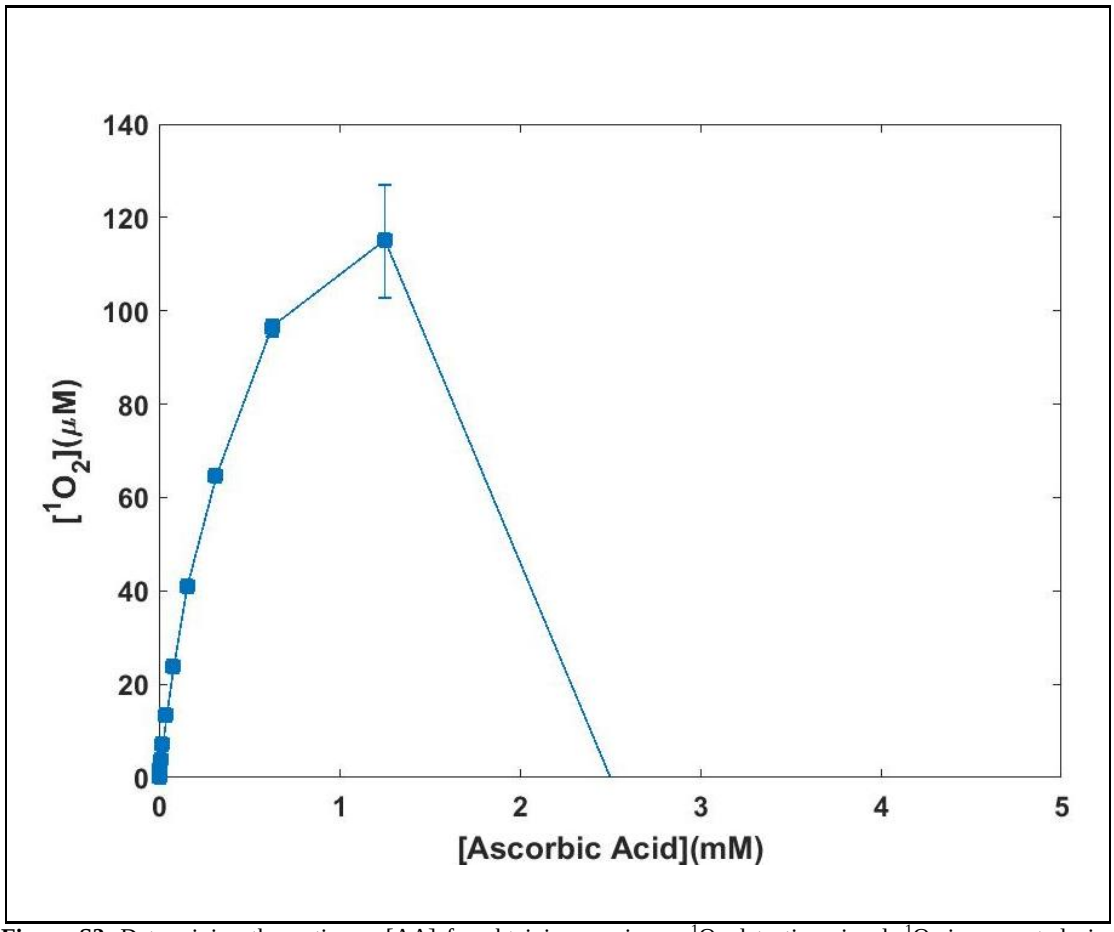

Figure S3. Determining the optimum [AA] for obtaining maximum $^1O_2$ detection signal. $^1O_2$ is generated via photosensitization reactions in solution.

4. Optimization of Ascorbic Acid for 15mg of RB-silica microparticles:

RB functionalized silica microparticles (RB-silica) was suspended in 1x DPBS (pH 7.4) to obtain a concentration of 15mg RB-silica per 100µL of suspension. Ascorbic acid (100µL, 10mM stock) was serially diluted in DPBS (pH 7.4, 100µL) with a dilution factor of 1/2 in 11 wells of a clear 96-well microplate. A well containing DPBS (pH 7.4, 100µL) was used as the negative control. RB-silica suspension (100µL, 15mg per 100µL of suspension) was added to all 12 wells. The plate was placed in the green-light illuminator and illuminated from the top for 30 minutes. 150µL of the supernatant from each well was collected in individual microcentrifuge tubes. The tubes were centrifuged in a microcentrifuge at 18000xg for 5 minutes. 100µL of the supernatant from the tubes were then transferred to a new clear 96-well microplate. An absorption spectrum was performed for all 11 wells using a plate reader to ensure there was no freely diffusing RB in solution. HRP (20µL, 0.171µM stock) and TMB (100µL, 1.04mM stock) were then added to each well. The plate was covered with aluminium foil and incubated for 5 minutes. The absorbance intensity at 650nm was measured for each well in a plate reader. The above experiment was performed in triplicate and each data point is reported as the mean $\pm$ S.E.M. The absorbance intensity at 650nm was converted to $[H_2O_2]$ using the H_2O_2 standard curve.

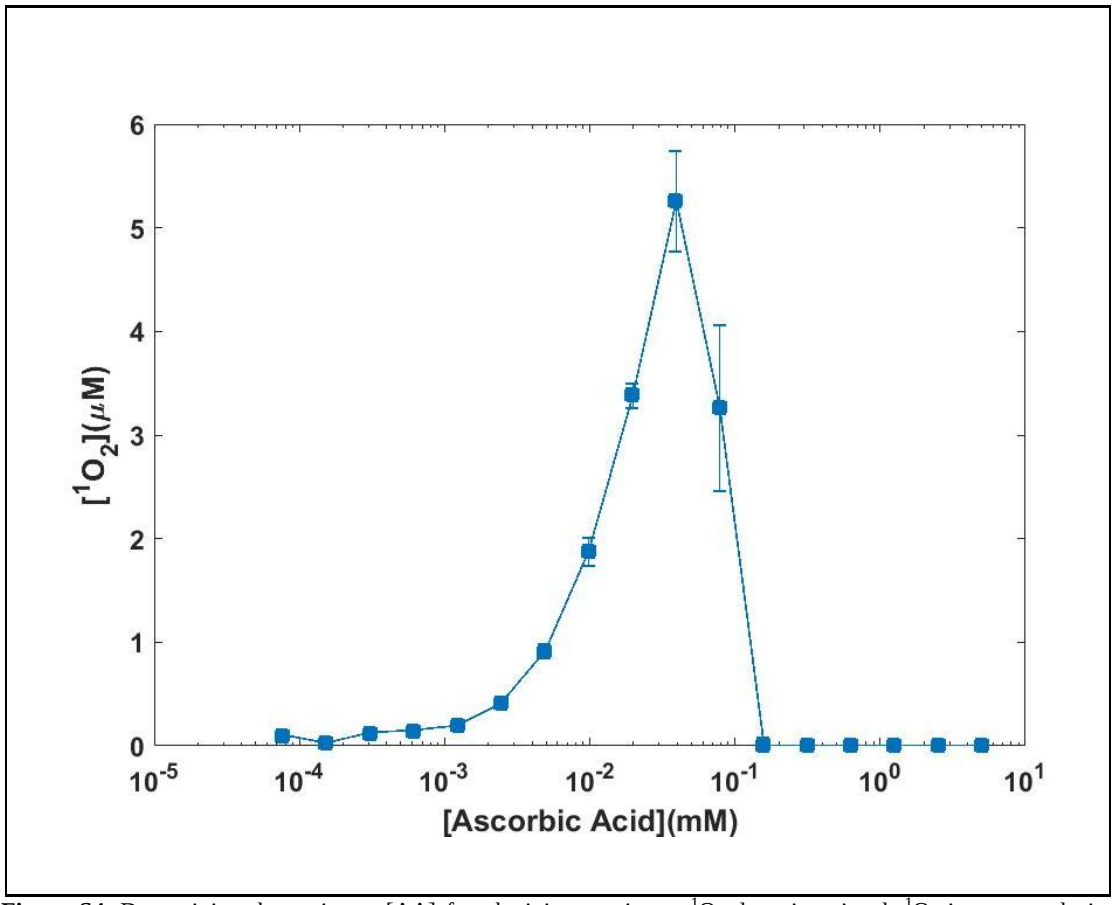

Figure S4. Determining the optimum [AA] for obtaining maximum $^1O_2$ detection signal. $^1O_2$ is generated via photosensitization reactions on a surface.

CHAPTER 3

CONCLUSION

We have developed a surface-based biosensor and showed specific capture of primary antibodies followed by generation of an antibody-dependent colorimetric signal via ACWOP. The sensor incorporates porous silica microparticles as an inexpensive substrate that is functionalized with ACWOP co-factors and an antigen. By eliminating secondary reagents, we have developed a universal platform that can be functionalized with a number of antigens to detect specific antibodies in a species-independent and inexpensive manner. This enables us to transition to a lateral flow assay based point-of-care device to detect Lyme antibodies against specific *Borrelia* antigens functionalized on the surface.

Future studies will involve utilizing our platform to functionalize histidine-tagged Lyme antigens such as OspA, OspC and OspF and directly detecting Lyme antibodies. Concurrently, efforts will be made to functionalize ACWOP cofactors and *Borrelia* antigens on nitrocellulose membranes, followed by capture and detection of Lyme antibodies via ACWOP on a lateral flow test strip. Development of the universal platform provided a deeper understanding of the chemistry involved in biosensing using the catalytic property of antibodies, which also gives insight into further upgrades of the sensor.

APPENDIX

A) Immobilization of biotinylated antibodies on a neutravidin coated plate followed by detection with ACWOP:

1. Optimization of [RB]:

(i) Determination of minimum moles of RB required to absorb the incident green light completely:

A serial dilution of 0.25mM RB stock was performed with dilution factor of 1/2 and a range of 0-0.25mM (100µL). Absorbance at 550nm was measured using a plate reader. Using Beer-Lambert's law, the Absorbance at 550nm was converted to fraction of green light absorbed using the formula: Fraction = $1-10^{-\text{Abs at 550nm}}$

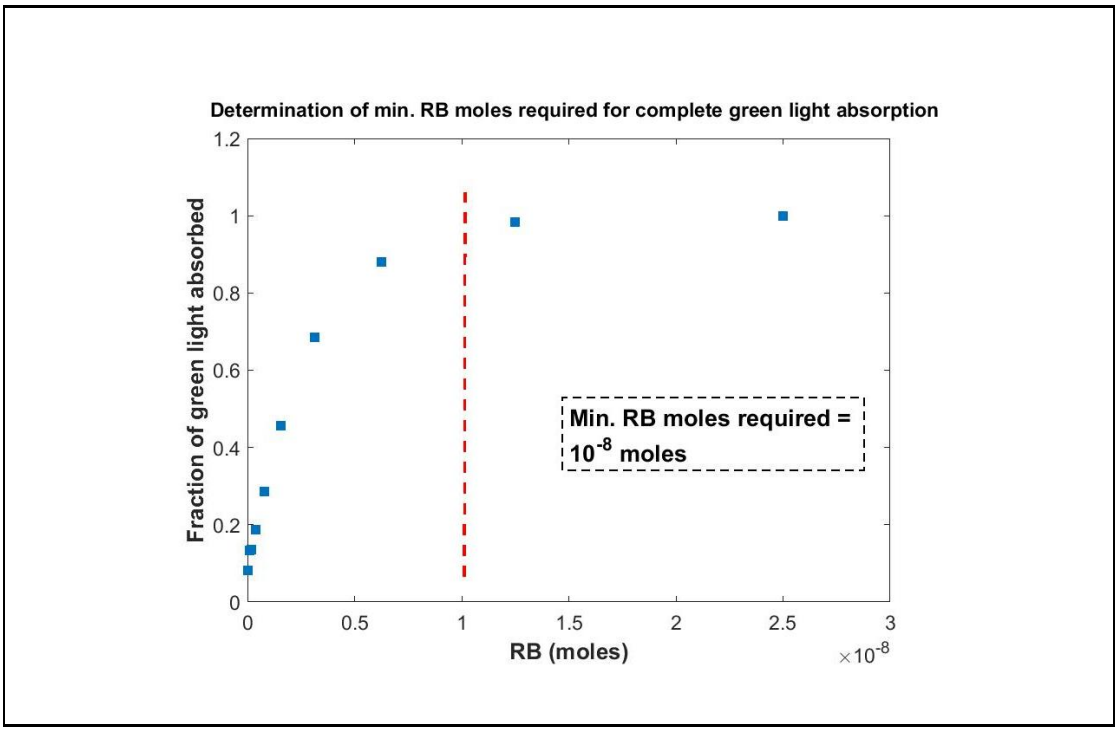

Figure A.1.1. Determining the minimum moles of RB required for complete absorption of green light. Observed that a minimum of 10^{-8} moles of RB was required.

(ii) Determination of molar absorption coefficient(ε) and characteristic length(L_C) at 550nm for RB:

A serial dilution of 0.1mM RB stock was performed with dilution factor of 1/2 and a range of 0-0.1mM (100µL). Absorbance at 550nm was measured using a plate reader. A plot of Abs/L at 550nm vs [RB] was developed and the slope of the curve provided the molar extinction coefficient (ε) of RB at 550nm. This value was used to calculate Lc or the attenuation length as a function of [RB] using the formula:

$$L_C = \frac{1}{2.303 \text{ x } [RB] \text{ x } \varepsilon}$$

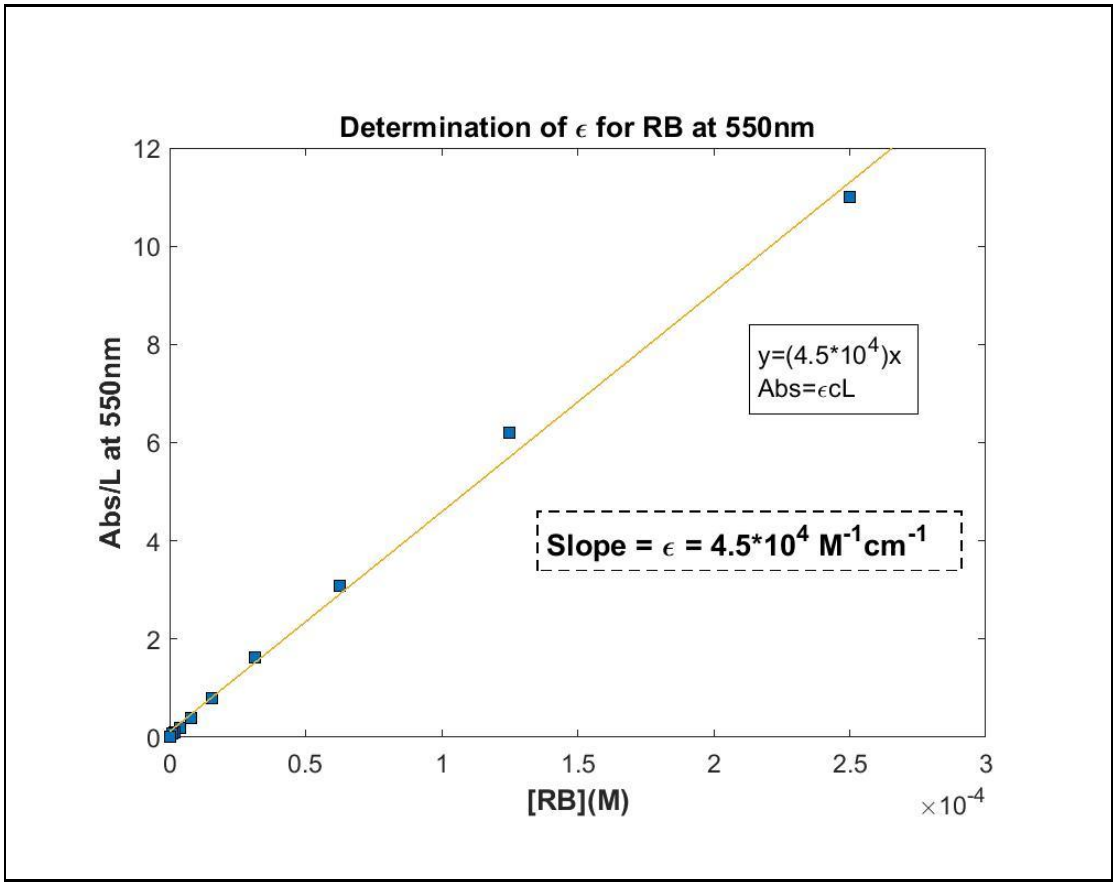

Figure A.1.2. Determining the molar absorption coefficient for RB at 550nm. Slope of Abs/L vs concentration curve gave the value of the coefficient.

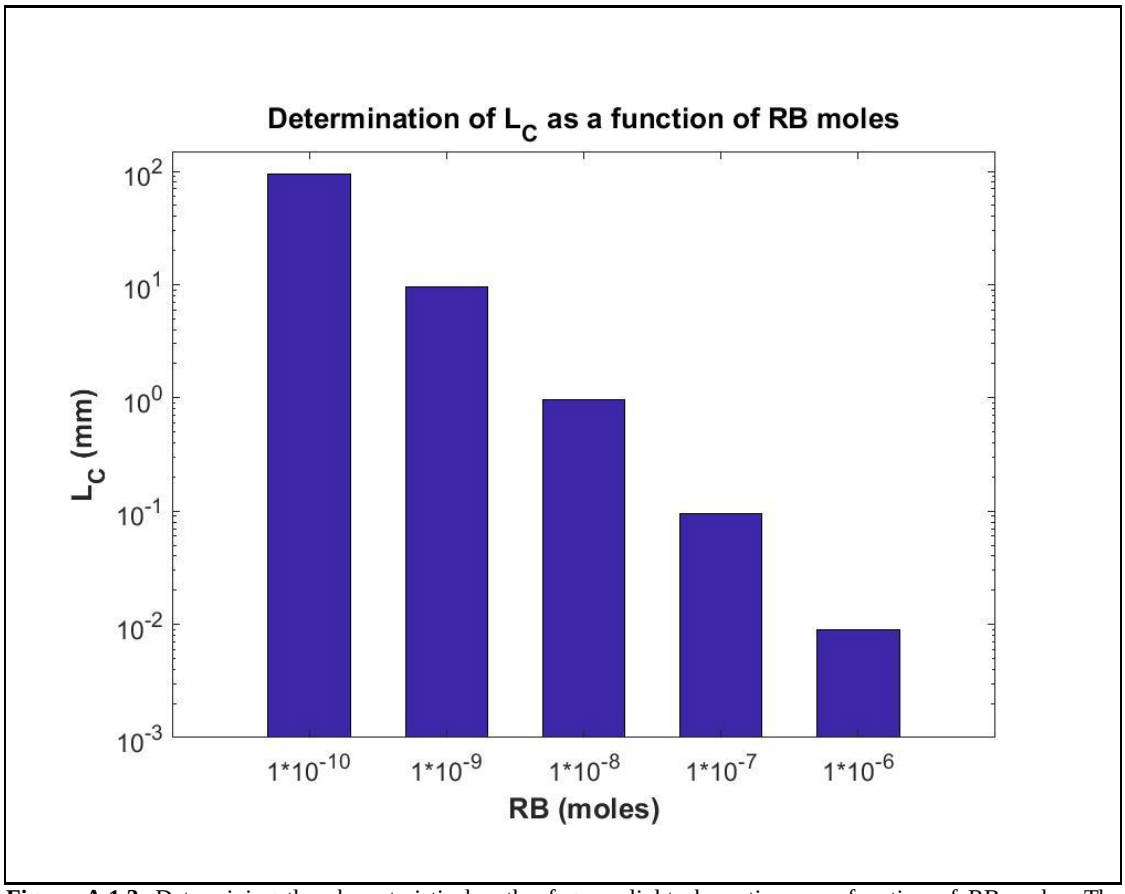

Figure A.1.3. Determining the characteristic length of green light absorption as a function of RB moles. The Length decreased as the RB solution became more concentrated.

(iii) Analysis of Limit of Detection(LOD) of H_2O_2 as a function of moles of RB in solution:

Five RB stock solutions were prepared – 0.01M, 1mM, 0.1mM, 0.01mM and 1uM. 100µL of each stock solution provides different number of moles of RB in solution. For each RB stock solution a H_2O_2 calibration curve was prepared. A H_2O_2 serial dilution was performed with dilution factor of 1/2 and a range of 0-20µM H_2O_2(100uL). 0.171µM HRP stock (20uL), 1.04mM TMB stock (100µL) and 100µL of RB was added to each well for every RB condition. After an incubation time of 5 minutes, absorbance at 650nm was measured and a calibration curve was plotted. The LOD was calculated from the plot using regression analysis and taking 3.3 times the

SNR (Signal to Noise Ratio). A table was prepared relating the Limit of Detection of each condition to the RB moles.

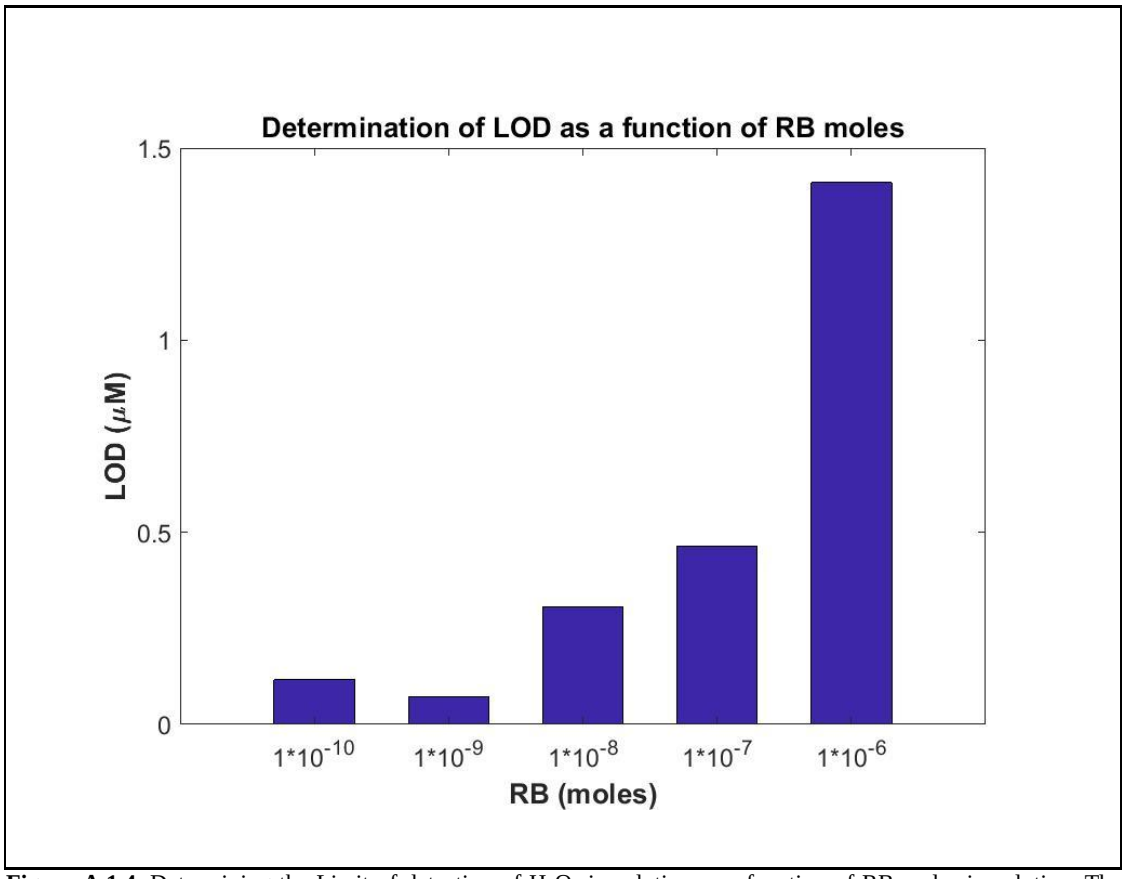

Figure A.1.4. Determining the Limit of detection of H_2O_2 in solution as a function of RB moles in solution. The LOD was best for RB = 10^{-9} moles.

Considering the above factors, [RB] = 0.2mM was chosen as the optimal concentration for the following experiment.

2. Immobilization of biotinylated goat and mouse IgG on neutravidin surfaces followed by readout with ACWOP

N-mouse IgG bound to biotin was purchased from Santa Cruz Biotechnologies with stock concentration of 2.67μM. A biotin - neutravidin chemistry was utilized to immobilize IgG on a surface. A serial dilution of IgG was performed with a dilution

factor of 1/2 and range of 0-2.67μM (100μL) in a clear 96-well plate. 95μL of the resulting solution was transferred to a neutravidin coated plate purchased from Thermo Fisher Scientific. The plate was cover with aluminium foil and incubated in an incubation shaker at 25^{o}C at a speed of 200 for 2 hours. After incubation, the wells were washed three times with wash buffer (0.05% Tween-20 in PBS) by gently squirting with a squirt bottle and subsequent flip-and-dry steps. 0.2mM RB stock (100μL) was added to each well. The plate was illuminated with green light from below for 45 minutes. 0.171μM HRP stock (20μL) and 1.04mM TMB stock (100μL) was added to each well and after 5 minutes, 215μL of solution from each well was transferred to another clear 96-well plate. Absorbance at 650nm was measured with a plate reader. A plot of Abs/L at 650nm vs [IgG] immobilized was developed to demonstrate an antibody dependent ACWOP signal from IgG immobilized on a surface. The same procedure was used with Goat anti-mouse IgG bound to biotin that was purchased from Santa Cruz Biotechnologies with stock concentration of 2.67μM.

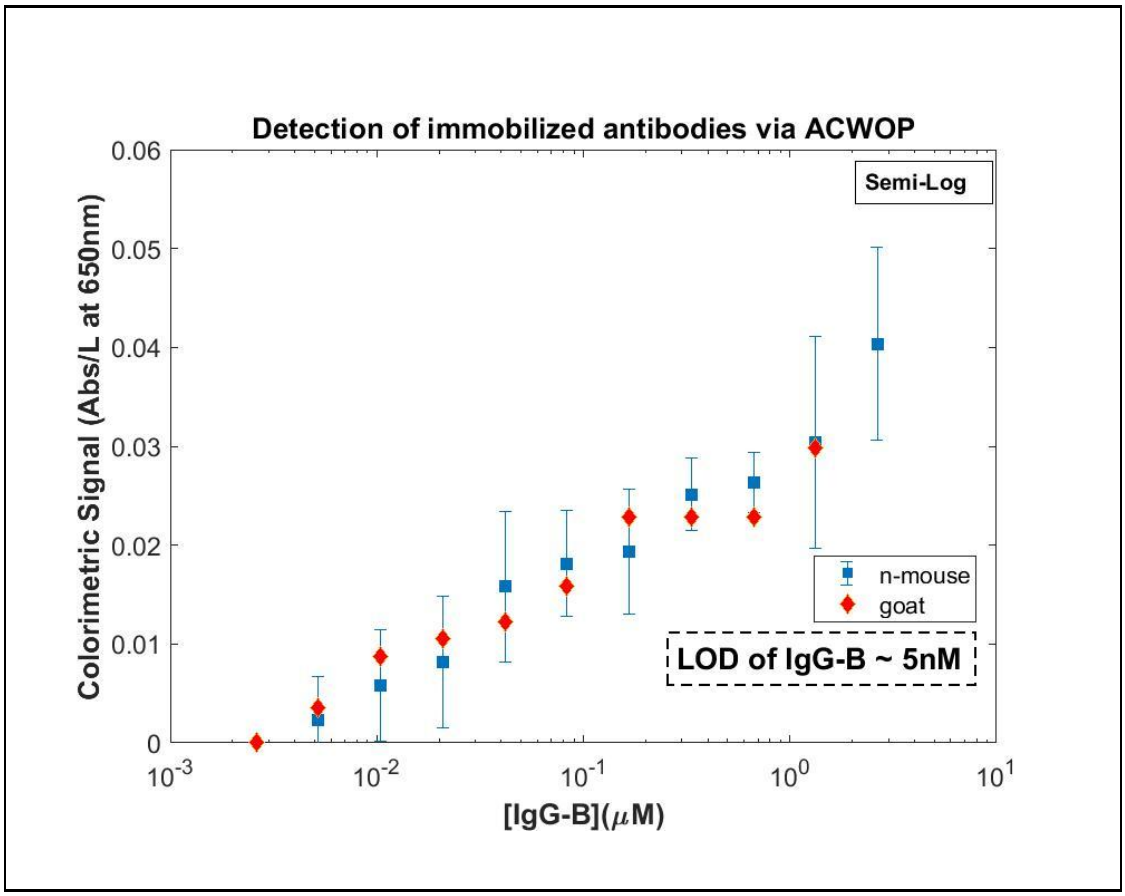

Figure A.2.1. Demonstration of detection of immobilized biotinylated antibodies on neutravidin surfaces via ACWOP. Obtained an antibody-dependent colorimetric detection signal. Two different antibodies- mouse and goat IgG were detected with the same assay thereby demonstrating species-independence

B) H_2O_2 standard curve for the immobilization of biotinylated IgG on neutravidin surfaces and readout with ACWOP signal:

H_2O_2 was detected by the oxidative color change of TMB in the presence of HRP. H_2O_2 (100µL, 64µM stock) was serially diluted in DPBS (pH 7.4, 100µL) with a dilution factor of 1/2 in 11 wells of a clear 96-well microplate. A well containing DPBS (pH 7.4, 100µL) was used as the negative control. RB (100µL, 0.2mM stock), HRP (20µL, 0.171µM stock) and TMB (100µL, 1.04mM stock) were added to all 12 wells. The plate was covered with aluminium foil and incubated for 5 minutes. The absorbance intensity at 650nm was measured using a plate reader for all the wells. The

above experiment was performed in triplicate and each data point is reported as the mean ± S.E.M.

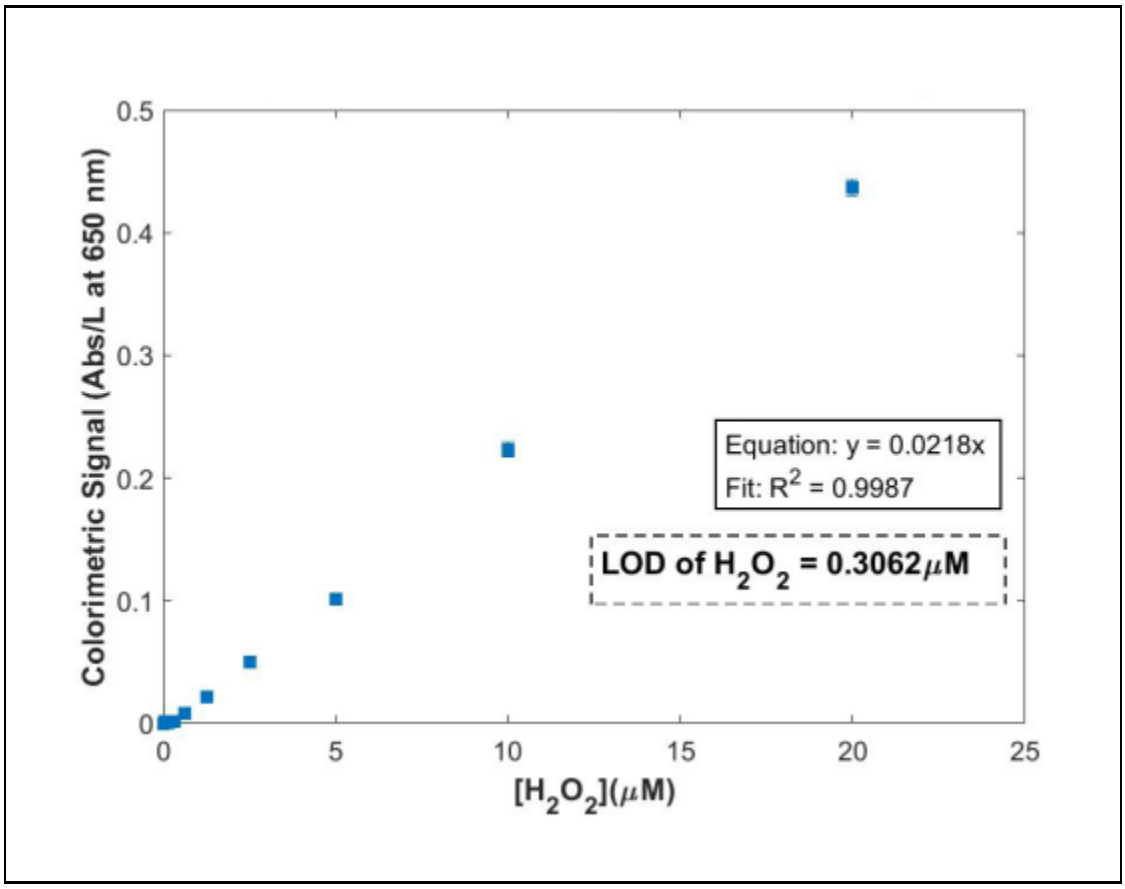

Figure B.1.1. H_2O_2 standard curve for detection of immobilized biotinylated antibodies on neutravidin surfaces via ACWOP. [RB] = 0.2mM, [TMB] = 1.04mM, [HRP] = 0.171μM and time = 5 minutes.

REFERENCES

[1] Eugene D. Shapiro; Clinical practice. Lyme disease.; The New England journal of medicine; 370(18):1724–31, 2014. ISSN 1533-4406. doi:10.1056/NEJMcp1314325.

[2] Lantos PM et. al.; Chronic Lyme Disease; Infect Dis Clin North Am.; 2015 Jun; 29(2):325-40. doi: 10.1016/j.idc.2015.02.006.

[3] Johnson.; Severity of Chronic Lyme Disease Compared to Other Chronic Conditions: A Quality of Life Survey.; PeerJ 2 (2014): e322. PMC.

[4] Coburn, Jenifer et al.; Illuminating the roles of the Borrelia Burgdorferi adhesins; Trends in Microbiology , Volume 21 , Issue 8; 372 – 379.

[5] G P Wormser, R J Dattwyler, E D Shapiro, J J Halperin, A C Steere, M S Klempner, P J Krause, J S Bakken, F Strle, G Stanek, L Bockenstedt, D Fish, J S Dumler, and R B Nadelman.; The clinical assessment, treatment, and prevention of lyme disease, human granulocytic anaplasmosis, and babesiosis: clinical practice guidelines by the Infectious Diseases Society of America.; Clin Infect Dis; 43(9):1089–1134; 2006. doi: 10.1086/508667.

[6] Stricker RB, Johnson L;. Let's tackle the testing.; BMJ : British Medical Journal. 2007; 335(7628):1008. doi:10.1136/bmj.39394.676227.BE.

[7] Manning, Colleen F., Angeliki M. Bundros, and James S. Trimmer.; Benefits and Pitfalls of Secondary Antibodies: Why Choosing the Right Secondary Is of Primary Importance.; Ed. Joy Sturtevant.; PLoS ONE 7.6 (2012): e38313. PMC. Web. 5 June 2018.

[8] Wentworth, P.; Jones, L. H.; Wentworth, A. D.; Zhu, X. Y.; Larsen, N. A.; Wilson, I. A.; Xu, X.; Goddard, W.A.; Janda, K. ; Eschenmoser, A.; Lerner, R. A.; Science; 2001; 293, 1806.

[9] Wagner et. al.; Antibodies to Borrelia burgdorferi OspA, OspC, OspF, and C6 antigens as markers for early and late infection in dogs; Clin Vaccine Immunol.; 2012 Apr; 19(4):527-35.

[10] Buxton Bridges C et. al.;Decreased antibody response among nursing home residents who received recalled influenza vaccine and results of revaccination, 1996-97.; Vaccine. 2000 Jan 6; 18(11-12):1103-9.